Conférence Internationale sur les Energies Vertes et le Traitement des Eaux

(EVE-2023)

Proceedings of Engineering & Technology

-PET-

Editor : Dr. Ahmed Rhif (Tunisia)

ICID

Centre International d'Innovation et de Développement

Proceedings of Engineering & Technology

-PET-

Conférence Internationale sur les Energies Vertes et le Traitement des Eaux

(EVE-2023)

Editor :
Dr. Ahmed Rhif (Tunisia)

PET-Vol. 79
ISSN : 1737-9334

Committees

Honorary General Chairs :

- Djamila Rekioua (ALG)
- Georges Descombes (FR)
- Rachid Benchrifa (MAR)

General Chairs :

- Ahmed Rhif (TUN)
- Benzeroual Tarek (ALG)
- El Mati Khoumri (MAR)
- Kasbadji Merzouk Nachida (ALG)

International Committee :

- Abdelfettah Barhdadi (MAR)
- Abdelkrim Khireddine (ALG)
- Abdellah Mechaqrane (MAR)
- Djeghlal Mohammed Elamine (ALG)
- Gasmi Ines (FR)
- Haitham Saad Mohamed Ramadan (FR)
- Jaafar Gaber (FR)
- Kamal Reklaoui (MAR)
- Karim Khireddine (ALG)
- Madiha Yessari (MAR)
- Manal Marzouq (MAR))
- Meriem HAYANI MECHKOURI (MAR)
- Mimi Belatel (ALG)
- Mohamed GHERBI (ALG)
- Nawel Seddiki (ALG)
- Rafika Boudries (ALG)
- Saida Derouiche (ALG)
- Sara Zatir (ALG)
- Selma Rabhi (ALG)
- Souad Tayane (MAR)
- Soukaina Akrouch (MAR)
- Toufik Madani Layadi (ALG)
- Touria Barradi (MAR)
- Youssef Errami (MAR)
- Zohra Ameur (ALG)

Summary

Towards Sustainable Agriculture: An Integrated Approach with a Hybrid PV/Wind/Battery System for Greenhouse Energy Management

Aymen LACHHEB [#1],Safa SKOURI, Sidi Mohammed El Amine BEKKOUCHE[*2], Salwa BOUADILA [**3]

[#] *Centre de Recherches et des Technologies de l'Energie, Thermal Processes Laboratory Technopole de Borj-Cédria, BP : 95, Hammam Lif, Ben Arous, Tunisia.*
** Laboratory Smart Electricity & ICT, SEICT, LR18ES44, National Engineering School of Carthage, University of Carthage, Tunisia.*
*** Unité de Recherche Appliquée en Energies Renouvelables, URAER, Centre de Développement des Energies Renouvelables, CDER, 47133, Ghardaïa, Algeria.*

Email 1 - salwa.bouadila@crten.rnrt.tn
Email 2 - aymen.lachheb1@gmail.com
Email 3 - smabekkouche@gmail.com

Abstract :

In this study, the authors propose an architecture for a hybrid energy generation system combining wind and photovoltaics. This system is designed to be easily connected or disconnected from the grid in order to manage energy surpluses or deficits. The authors also connect a PV/Wind/Battery hybrid installation to an already grid-connected hydroponic greenhouse. This allows them to reduce the amount of energy consumed from the grid. The authors conclude that this shift from traditional energy sources to renewable sources will have a positive impact on the environment and can also contribute to reducing the bimonthly energy bill of the hydroponic greenhouse

I. Introduction :

The exploitation of photovoltaic solar energy provides a good solution for generating electricity. The efficiency of renewable energy sources depends on climatic conditions. Indeed, a single source of renewable energy sometimes cannot provide the required energy. In such cases, hybrid systems combining two or more renewable energy sources offer a safe and effective solution to address this dependence on renewable energies [1]. Therefore, there are several topologies of hybrid installations. Among them, we can mention PV/wind [2], PV/wind/battery [3], PV/wind/fuel cell/battery [4], and wind/battery [5]. The combination of multiple renewable energy sources of different natures minimizes the effect of energy production discontinuity, particularly when combined with a storage system. However, this requires attention to many fundamental factors, such as the management of energy production and storage. This is especially crucial given the high cost of the storage system, which represents a major constraint in the overall cost. This necessitates an energy management strategy to optimize production capacity, minimize storage costs, and protect the battery against deep discharges and overloads [6].

This work presents a control strategy based on multiple scenarios to ensure an optimal distribution of energy among different sources and effectively meet the specific electrical needs of hydroponic

ISSN: 1737-9334

greenhouses. This approach proposes dynamic energy management, allowing for the maximization of the use of various available energy sources while ensuring a reliable and sustainable power supply. A thorough numerical analysis is conducted on three integrated systems within the setup to meet its electrical requirements. The study focuses on three different scenarios: the first option is a photovoltaic power plant connected to the grid, the second is a wind turbine connected to the grid (Figure 1), and the last is a hybrid PV/Wind/Battery system (Figure 1).

II. Materials and methods :

Figure 1 illustrates the suggested hybrid installation structure, including the directions of energy flows and the energy management system. To optimize the best configuration of the hybrid system that meets the requirements of the hydroponic greenhouse, three scenarios were studied:

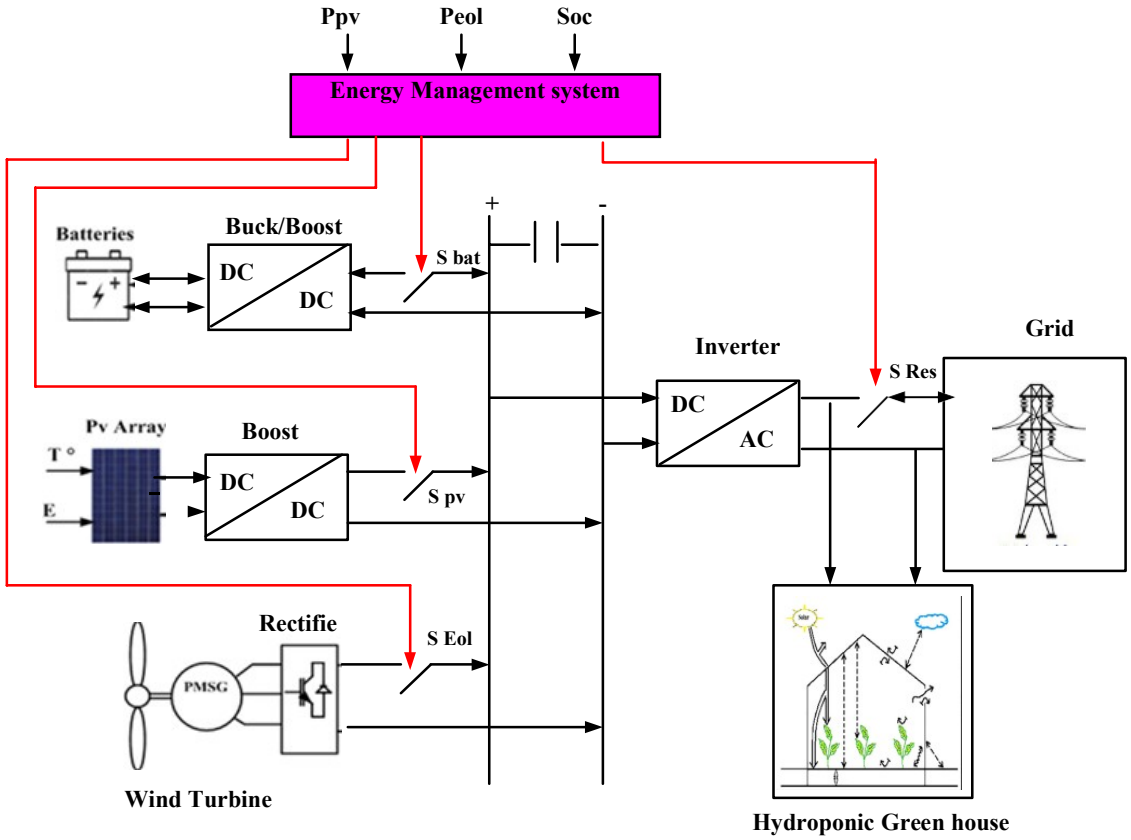

Figure 1: components of hybrid PV wind battery system

III. Modelling of hybrid system:

1. Modelling of PV system

The solar converter consists of a solar PV panel, and a DC-DC boost converter with MPPT controller as shown in Fig. 2. In essence, a photovoltaic cell can be likened to an electrical current generator shunted with a diode. This diode is created through the formation of a p–n junction. To delve into the physical phenomena occurring within the cell, the model incorporates two intrinsic resistors, *Rs* and *Rp*, in series and parallel arrangements, as depicted in Figure 2.

ISSN: 1737-9334

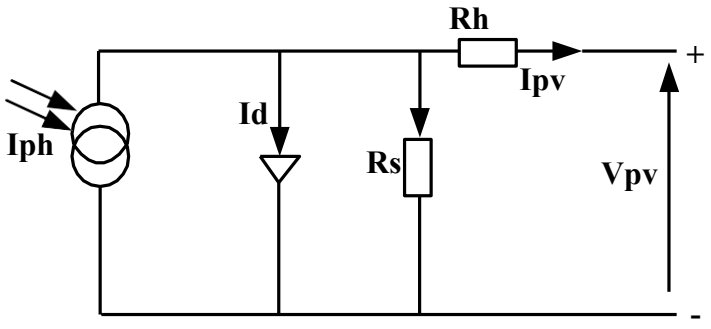

Figure 2: equivalent diagram of photovoltaic panel

A photovoltaic generator is composed of a collection of individual photovoltaic cells interconnected in series and/or in parallel. Consequently, the following equation describes the current output delivered by the PV panel as a function of the number of cells in series (Ns) and in parallel (Np) [7]:

$$I_{pv} = N_p I_{ph} - N_p I_s \left[\exp\left(\frac{V_{pv} + R_s I_{pv}}{n V_{th}}\right) - 1 \right] - N_p \left(\frac{V_{ph} + R_s I_{pv}}{R_p}\right) \quad (1)$$

The proposed boost converter in shown in figure 3.

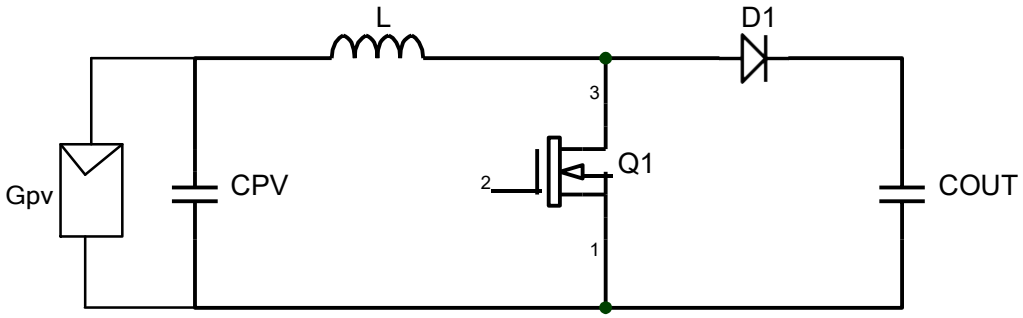

Figure 3: Boost converter the proposed system

The P&O method is used for maximum power extraction, the developed MPPT algorithm keeps the PV panel voltage near to MPP voltage to adjust the duty cycle (D). Then, the required change in duty cycle (ΔD) is calculated based on the change in voltage (ΔV) and the change in power (ΔP) [8].

2. Modelling of wind generator

The electrical model of the Permanent Magnet Synchronous Generator (PMSG) can be represented in the park reference frame as:

$$\begin{cases} u_d = R_s i_d + \dfrac{d\psi_d}{dt} - \omega_e \psi_q \\ u_q = R_s i_q + \dfrac{d\psi_q}{dt} + \omega_e \psi_d \end{cases} \quad (2)$$

The terms ψ_d and ψ_q delineate the integrated fluxes in each phase and can be defined as follows:

ISSN: 1737-9334

$$\begin{cases} \psi_d = L_d i_d + \psi_m \\ \psi_q = L_d i_d \end{cases} \quad (3)$$

In the context of a permanent magnet synchronous generator (PMSG), L_d and L_q represent the stator inductances in the d-q reference frame, while ψ_m characterizes the rotor flux of the generator. The electromagnetic torque of the PMSG can be computed by utilizing the expression for electromagnetic power, as defined in Equation (4).

$$P_e = \omega_{me} T_e = \frac{3}{2} \omega_e (\psi_d i_q - \psi_q i_d) \quad (4)$$

The electromagnetic torque can be derived as:

$$T_e = \frac{3}{2} \frac{p}{2} (\psi_d i_q - \psi_q i_d) \quad (5)$$

3. Battery storage system

The storage system comprises a lead-acid battery and a bidirectional DC-DC buck-boost converter. This converter utilizes a PI controller, as depicted in Figure 3, to regulate the DC bus voltage [9].

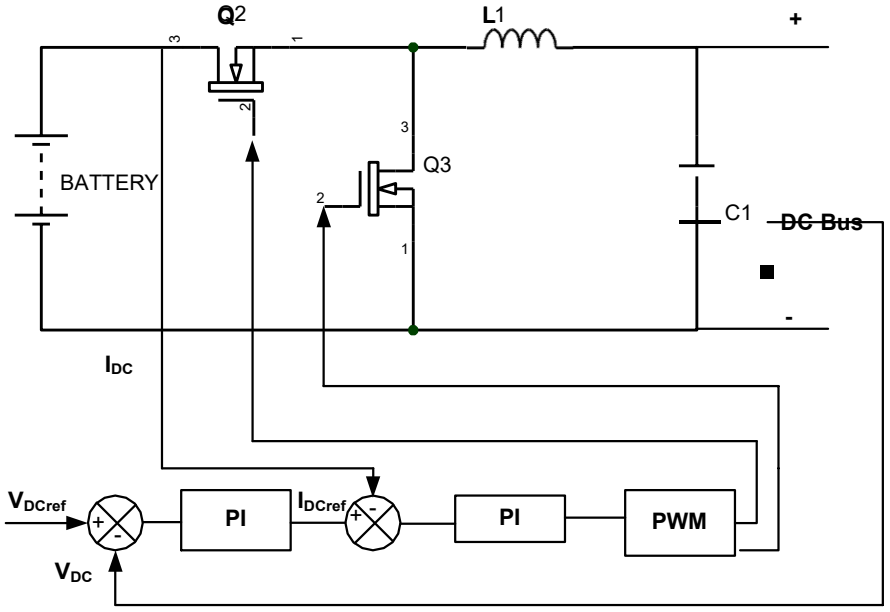

Figure 4: Buck boost converter

Results:

The simulation was conducted assuming that the batteries were initially charged ($SOC = SOC_{max}$), with a value of approximately 95%. Figure 5 illustrates the power of the hybrid production system connected to the grid. The simulation results demonstrate that the battery exhibits dynamic behavior, responds efficiently to load requirements, and ensures a continuous energy supply even without production from the hybrid system. During the period from 00:00h to 05:00h, when the hybrid system does not generate electricity, the storage system's battery continues to provide the necessary energy to meet the energy needs of the hydroponic greenhouse. From 5:00

ISSN: 1737-9334

AM onward, the hybrid system begins to supply energy, and the batteries start to charge. At this point, the system exports surplus energy to the grid.

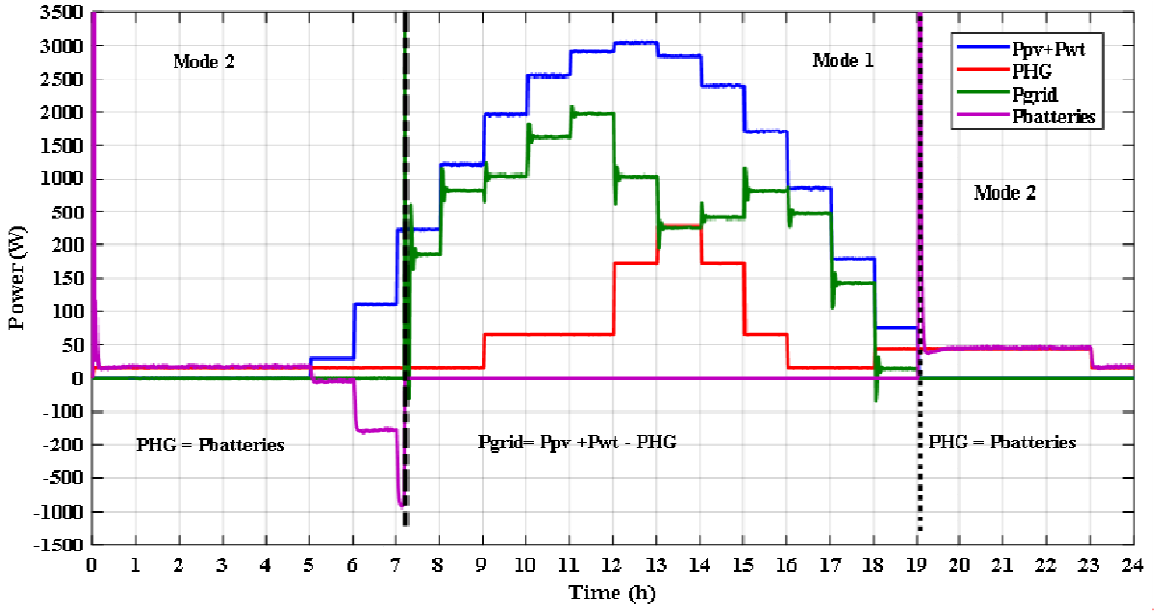

Figure 5: Power of the hybrid system with an initially charged battery

The Figure 6 represents the variation in battery voltage over a complete cycle. The results show that during the discharge phase, the battery voltage decreases, indicating the use of stored energy. However, as soon as the hybrid system starts generating sufficient energy, the batteries recharge, causing the voltage to increase until it reaches its maximum value. This behavior confirms the dynamic response of the batteries, adapting to the hybrid system by adjusting energy production levels and efficiently managing the charge and discharge process to maintain optimal voltage levels.

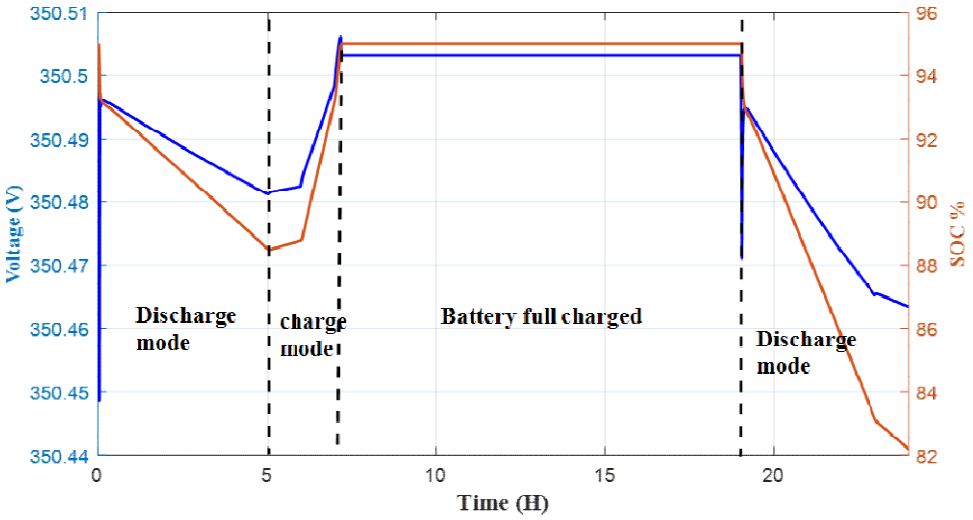

Figure 6 *:* Variation of battery voltage and state of charge over time

ISSN: 1737-9334

Conclusion :

In this work, a hybrid PV/Wind/Battery system is employed. To assess the performance of the hybrid system for supplying electricity to a hydroponic greenhouse, modeling and simulation are conducted over a day. Subsequently, an Energy Management System (EMS) is designed to ensure the optimal management of this energy system. The EMS oversees the renewable energy source's energy management to meet the greenhouse's energy needs while considering the power phase shift between the load's demand and that produced by the PV/Wind/Battery hybrid system.

The use of an Energy Management System (EMS) has contributed in several ways to the energy management of a hybrid system, including:

-Maximizing the use of renewable energies, thereby reducing the system's dependence on the electrical grid.

-Efficient energy storage: The EMS algorithm has determined the optimal time for charging and discharging batteries, thereby maximizing the use of stored energy during periods of low renewable energy production or high electricity demand.

Références :

[1] Delalay S. Étude systémique pour l'alimentation hybride – application aux systèmes intermittents. vol. 5768. École Polytechnique Fédérale de Lausanne.: 2013.

[2] Amorndechaphon D, Premrudeepreechacharn S, Higuchi K, Roboam X. Modified grid-connected CSI for hybrid PV/wind power generation system. Int J Photoenergy 2012;2012. https://doi.org/10.1155/2012/381016.

[3] Khan MJ, Yadav AK, Mathew L. Techno economic feasibility analysis of different combinations of PV-Wind-Diesel-Battery hybrid system for telecommunication applications in different cities of Punjab, India. Renew Sustain Energy Rev 2017;76:577–607. https://doi.org/10.1016/j.rser.2017.03.076.

[4] Fathabadi H. Novel standalone hybrid solar/wind/fuel cell/battery power generation system. Energy 2017;140:454–65. https://doi.org/10.1016/j.energy.2017.08.098.

[5] Sarrias R, Fernández LM, García CA, Jurado F. Coordinate operation of power sources in a doubly-fed induction generator wind turbine/battery hybrid power system. J Power Sources 2012;205:354–66. https://doi.org/10.1016/j.jpowsour.2012.01.005.

[6] Adouane M, Haddadi M, Medjoudj R. Conception et réalisation d'un module électronique de contrôle et de gestion optimale de l'énergie pour systèmes énergétiques hybrides photovoltaïque - groupe électrogène. Rev Des Energies Renouvelables 2011;11:9–15.

[7] Alshebli, R. F., & Bicer, Y. (2022). Energy and exergy analysis of a renewable energy-driven ion recovery system for hydroponic greenhouses. Sustainable Energy Technologies and Assessments, 53, 102628.

[8] Roumila, Zoubir, Rekioua, Djamila, et Rekioua, Toufik. Energy management based fuzzy logic controller of hybrid system wind/photovoltaic/diesel with storage battery. International Journal of Hydrogen Energy, 2017, vol. 42, no 30, p. 19525-19535.

[9] Bortolini, Marco, GAMBERI, Mauro, et GRAZIANI, Alessandro. Technical and economic design of photovoltaic and battery energy storage system. Energy Conversion and Management, 2014, vol. 86, p. 81-92.

ISSN: 1737-9334

Enhancing Wind Farm Monitoring and Analysis: Cloud Infrastructure Deployment, System Maintenance, and Automation

Amel Jelidi[*#, 1], Mohamed Elleuch[*, 2],Tzu-Yun Weng[#], Siti Winny Maulidiani[#, 3], Luthfi Irawan Prihatmadi[#]

[*]*University of Tunis El Manar, ENIT-LSE, LR11ES15, B.P 37 Le Belvédère, 1002 Tunis, Tunisia*
[#]*BayWa r.e. APAC, Wind Engineering Department, Wind Resource Analysts Team*

Email 1 –amel.jelidi@etudiant-enit.utm.tn
Email 2 –Mohamed.elleuch@enit.utm.tn
Email 3 –sitiwinny.maulidiani@baywa-re.com

Abstract:

This study was conducted with the aim of uncovering the intricacies and prospects of Wind Data Forecasting & Infrastructure. This endeavor harbored the deployment of a cloud infrastructure for 8 metmasts across the Asia Pacific Region (APAC) with Microsoft Azure along with the investigation and automation of four wind data management basic functionalities: monitoring, cleaning, report creation & Long-term (LT) Analysis. The LT Analysis was built on the Measure Correlate Predict (MCP) architecture where a Linear Least Squares model was defined and evaluated. The venture was concluded with the deployment of an all-encompassing infrastructure for the management of future wind site operations.

Keywords: Wind Resource Analysis, Long-Term Analysis, Microsoft Azure, Internet of Things.

I. Introduction

As the world seeps into an ever-approaching energy crisis, renewables have found themselves as the center of global, economic, and corporate interest [8].While occupying 5% of the global energy share, the wind energy market is nonetheless projected to reach $211.85bn by2030[9][11]. We have thus delved into the APAC market where 10 GW farms are currently poweringhouseholds & industries [7].

Despite the global momentum of wind farm development projects, grid integration may be the greatest contemporary challenge facing wind professionals nowadays due to strict grid codes and little to no visibility [10]. Companies such as BayWa r.e aim to close such a gap by investing in wind analysts to help with the different phases of project development.

Reducing the unpredictability ofwind energy yieldsis dependent on a plethora of variables, most notably: *wind*itself. Wind is not only an unpredictable meteorological element, but also requires constant monitoring to integrate the wind farms it powers. While a wind analyst is pivotal to the assessment of a given land plot's long-term potential and in spite of the development of Internet of Things (IoT) capacity, a lot of the wind data management tasks are far from automated.

II. Challenges to Address

This endeavor was the fruit of many years of inefficient and tedious work for the employees. While the team is composed of wind experts, there is a certain limit to the number of farms a group of people can manage. It is therefore essential to **automate, optimize & diversify**the capabilities of the system at hand. We may, thus,summarize our motivation under the following:

ISSN: 1737-9334

- Can we improve and automate wind data processing using IoT technologies?
- How can we make wind data & reports more accessible and centralized?
- How can we perform the LT analysis independently of third-party software?
- Are there alternatives to traditional LT algorithms?

There is a plethora of papers offering an overview of wind prediction methodologies and their intricacies such as A. Tascikaraoglu & M. Uzunoglu's 2014 encapsulation of individual and hybrid methodologies towards forecasting wind power [1].A good literature overview may also be that of Lawan et al. where different technologies, paper and metrics were showcased [5]. Common metrics such as the Mean Absolute Error (MAE), Mean Absolute Percentage Error, and others were projected across a multitude of technologies and resampling periods.

The growth in 5G technology has ignited discussions of digital twin technology where an asset can have a real-time digital copy that is both physical and signal-base. The 2023 IEEE conference on Power Electronics and Renewable Energy was presented with a paper on Wind Turbine Digital Twin based on Microsoft's Azure cloud services [4]. The paper explored Azure's potential when it comes to building digital twins and the forecasting of powerproduction.

III. Methodology

1. Daily Wind Data Monitoring

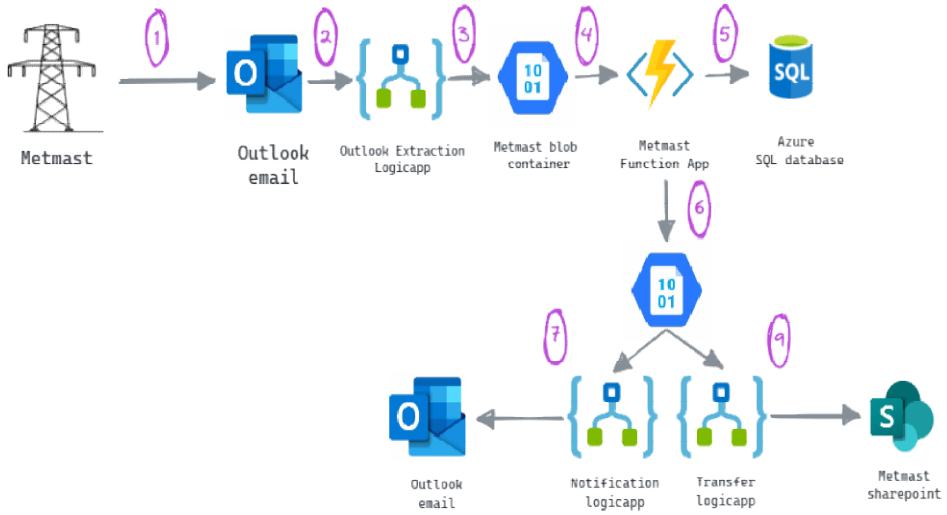

Figure 1: Azure-basedwind data monitoring system architecture

With eight metmasts across the Asia Pacific region (APAC), the daily monitoring and diagnostics of wind data and relevant sensors becomes a tedious and monotone task which calls for the automation of the overall process. We have thus created and maintained a fully automatic cloud-based wind data monitoring system, as seen under figure 1, capable of:

- Collecting sensor measurements from emails through the means of and Azure Logic App
- Storing the data in a dedicated Postgres database for analytics through an Azure Function App
- Transferring daily 'csv' files to relevant employees via an Azure Logicapp anda SharePoint
- Sending email alerts in cases of:
  - Low sensor correlation
  - Low battery levels which may hinder metmast functionalities.

ISSN: 1737-9334

2. Wind Data Cleaning

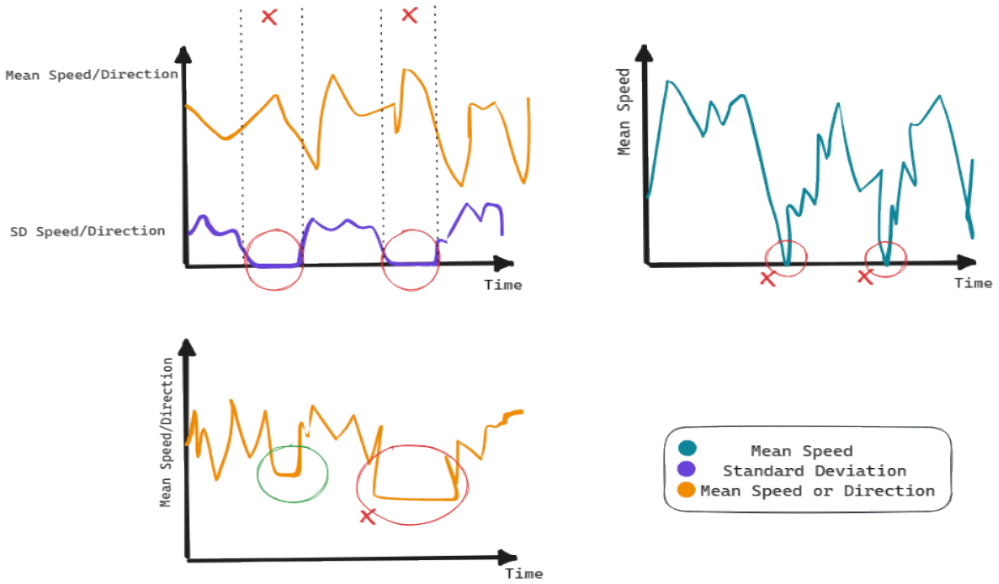

Figure 2: Common raw wind data defects to be removed.

Due to a plethora of factors, raw wind data is not available for direct use as seen under figure 2, we have thus overturned the time-consuming cleaning process through an Azure function that performs the following:

- Eliminating data with null Standard Deviation
- Ruling out null wind speed data
- Removing flatlines
- Reducing or eliminatingdata impacted by the shadow effect on given sensors.

These discrepancies are generally due to faulty sensors and will need intervention upon their persistence. Through the means of our cleaning function app, we are able to reduce their impact on analytics.

3. Monthly Report Generation

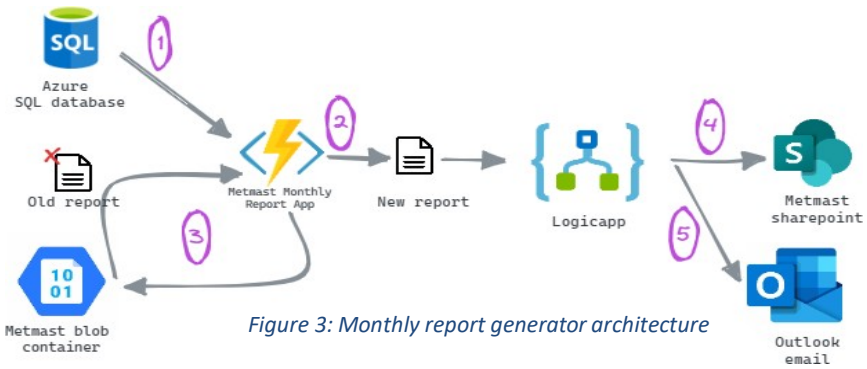

Figure 3: Monthly report generator architecture

Wind analysis requires extensive reporting which takes up 2 business days per month at the very least. To reduce these wasted resources, we harnessed the capabilities of Azure function apps under Figure 3 to

ISSN: 1737-9334

craft new reports for each month while also including data from past reports. The resulting document summarizes wind speed and sensor coverage for each month since the metmast has been set up.

4. Long Term Analysis

By following the Measure Correlate Predict methodology for the Long-term (LT) projection of the wind speed of a given site, we are capable of conservatively predicting the site's available wind resources.

a. Data Preparation

We resorted to 10 neighboring ERA-5 and MERRA-2 satellite metrology dataset sites per metmast to help find a trustworthy correlation between onsite and reference data[2, 3].While onsite metmasts have been performing measurements over a few months, reference data would include records from 2003. We then performed several resampling operations (daily, weekly, ten days and monthly) for six onsite metmastsand each of their 10 relative reference sites. In order to prevent bias, we ought to ensure that the data found within each timestep is representative of the overall sample. We have therefore enforced a minimum coverage rate pertimestep length along with obligatory timestep alignment of all involved datasets (onsite and reference).

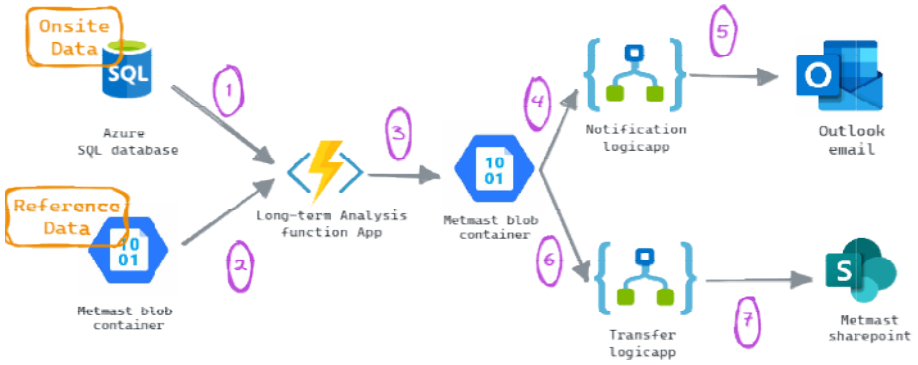

Figure4: LT Analysis Architecture

b. Model & Architecture building

S.M. Weekes & A.S. Tomlin studied the Measure Correlate Predict method using an LLS model showcasing a 0.21(m/s) MAE for only 3 months of data and 0.12(m/s) for 12 months [6]. We have thus opted for testing this model out as we aim for an architecture that requires minimal computing capabilities as the model will be running fully on the cloud as seen under figure 4. We will, thus, create 10 different models where the**output**is the ***onsite***wind speed, and the ***input*** is a **reference** wind speed.

IV. Results & Discussion

ISSN: 1737-9334

1. Automation

Upon deployment, 8 runs are generated daily which is directly equivalent to the number of metmasts. In fact, we have one daily run per metmast in the most perfect conditions and designated employees receive notification emails if data errors are found. Data cleaning is also accomplished on a daily basis and data is stored in a separate database. A monthly report may now be generated and may contain:

- Speed mean per month per year
- Cross-year speed mean of a given month (note that there are only 12 options)
- Speed coverage per month per year per sensor
- Direction coverage per month per year per sensor
- Overall coverage per sensor

2. LT Analysis

The following results provide the R^2 and mean od monthly means (MOMM) estimation provided by our LT analysis algorithm for sites across Asia.

Table 1: Model Monthly Forecast Performance

a. Monthly Projections

Onsite Metmast	Months	Mean R^2	MOMM Speed
”U”	9	0.852495	5.622321
”V”	9.5	0.944497	6.751833
”H”	20	0.623009	5.807894
”S”	12	0.635339	5.79401
”R”	25	0.776146	6.311221

Upon looking into the given results under Table 1, we noticed a variation in the performance metrics from site to sitewhere theR^2 was as high as 0.94 and as low as 0.62. This leads us to conclude that the model is site dependent, and tests have to be conducted prior to using it in future predictions. A pair of sites may not correlate at all due to geographic conditions or distance.

b. 10-day Projections

Table 2: Model 10-day Forecast Performance

Onsite Metmast	10-day sets	Mean R^2	Mean of 10-day Speed
”U”	30	0.804395	5.63136
”V”	30.5	0.913378	6.77554
”H”	57	0.398874	5.865808
”S”	37	0.567483	6.34979
”R”	83	0.625762	6.311221

As one observes the results under table 2, one can see acceptable R^2 rates for 10-day periods. We may also note a drop in accuracy in comparison to the monthly results, which is intuitive.

c. Weekly Projections

Onsite Metmast	Weeks	Mean R2	Mean of Weekly Speed
”U”	43	0.763164	5.663273

ISSN: 1737-9334

”V”	43.5	0.913816	6.777427
”H”	89	0.369586	5.883744
”S”	53	0.445704	5.817242
”R”	130	0.57236	6.266987

Table 3: Model Weekly Forecast Performance

In spiteof the satisfactory results for sites ‘V’ and ‘U’, all other sites under Table 3 showcase a serious drop in accuracy thus making the model untrustworthy for weekly projections as it is quite difficult to forecast a given week by merely using long term data.

Table 4: Model Daily Forecast Performance

d. Daily Projections

Onsite Metmast	Days	Mean R2	Mean of Daily Speed
”U”	307	0.73031	5.622321
”V”	327	0.86469	6.751833
”H”	730	0.271063	5.807894
”S”	379	0.418989	5.817242
”R”	1243	0.360944	6.266987

In spite of a surprisingly high R^2 rate for sites’U’ and ‘V’, the daily forecast results under Table 4are non-conclusive for daily long-term predictions which is typical for an MCP model.

e. Discussion

The results presented throughout this section showcased the strengths and weaknesses of our model to which we suggest possible remedies:

- Capabilities:
  - High Accuracy for Monthly and 10 Day timesteps
  - requires low computation power which is essential for cloud deployment.
- Limitations:
  - Low resolution for weekly and daily forecasts: *predicting such a short window through LT showcases low results in all literature as wind is hardly that predictable.*
  - Site Dependency: *the greatest weakness of this model and requires testing prior to fully adoptinga given site’s LT results.*

Conclusion:

Throughout the course of this endeavor, we aimed to reduce the wasted resources inflicted by thedifferent phases of wind data processing which results in low visibility and high dependence on external software. We have thus established a cloud-based monitoring, cleaning and reporting system. We have also dwelled on improving the pre-existing forecasting model and aim to test further long-term models along with short-term prediction methods.

References:

ISSN: 1737-9334

[1] A. Tascikaraoglu and M. Uzunoglu, "A review of combined approaches for prediction of short-term wind speed and power," Renewable and Sustainable Energy Reviews, vol. 34, pp. 243–254, 2014. [Online]. Available: https://www.sciencedirect.com/science/article/pii/S1364032114001944

[2]H. Hersbach et al., "The era5 global reanalysis," Quarterly Journal of the Royal Meteorological Society, vol. 146, no. 730, pp. 1999–2049, 2020. [Online]. Available: https://rmets.onlinelibrary.wiley.com/doi/abs/10.1002/qj.3803

[3] R. Gelaro et al., "The modern-era retrospective analysis for research and applications, version 2 (merra-2)," Journal of Climate, vol. 30, no. 14, pp. 5419 – 5454, 2017. [Online]. Available: https://journals.ametsoc.org/view/journals/clim/30/14/jcli-d-16-0758.1.xml

[4] R. Issa, M. S.Hamad, and M. Abdel-Geliel, "Digital twin of wind turbine based on microsoft® azure iot platform," in 2023 IEEE Conference on Power Electronics and Renewable Energy (CPERE), 2023, pp. 1–8.

[5] S. Lawan, W. Abidin, W. Chai, A. Baharun, and T. Masri, "Different models of wind speed prediction; a comprehensive review," International Journal of Scientific & Engineering Research, vol. 5, no. 1, pp. 1760–1768, 2014.

[6] S. Weekes and A. Tomlin, "Comparison between the bivariate weibull probability approach and linear regression for assessment of the long-term wind energy resource using mcp," Renewable Energy, vol. 68, pp. 529–539, 2014. [Online]. Available: https://www.sciencedirect.com/science/article/pii/S0960148114001013

[7] IEA, "ASEAN total installed wind capacity, 2017-2025," Tech. Rep., 2023. [Online]. Available: https://www.iea.org/data-and-statistics/charts/asean-total-installed-wind-capacity-2017-2025

[8] IEA, "Renewable Energy Market Update," Tech. Rep., 2023. [Online]. Available: https://www.iea.org/reports/renewable-energy-market-update-june-2023

[9] IEA. World gross electricity production by source, 2019. Technical report, 2023.

[10] Pramod Jain and Priyantha Wijayatunga, Asian Development Bank, "GRID INTEGRATION OF WIND POWER BEST PRACTICES FOR EMERGING WIND MARKETS," Tech. Rep., 2016. [Online]. Available: https://www.adb.org/publications/grid-integration-wind-power-best-practices-wind-markets

[11]Precedence research (2023). wind energy market. [online] available at: https://www.precedenceresearch.com/wind-energy-market [accessed 21 aug. 2023].

ISSN: 1737-9334

Thermal behavior of mortar incorporated with natural and textile fibers

Amira DELLAGI [#1], Rabeb AYED[#1], Safa SKOURI[#1], Salwa BOUADILA[#1], AmenAllah GUIZANI[#1]

[#1] *Centre de Recherches et des Technologies de l'Energie, Technopole de Borj-Cédria, BP : 95 Hamam Lif, Ben Arous, Tunisia*

Email 1 - amira.dellagi2@gmail.com

Email 2 - ayedrabeb09@gmail.com

Email 3 - amenallah.guizani@crten.mesrs.tn

Abstract:

This study seeks to assess the thermal efficiency of mortars in the construction sector by incorporating human hair and textile fibers. The objective is to achieve enhanced energy efficiency. The investigation involves substituting sand with fractions ranging from 10% to 50% in volume. The evaluation encompasses both thermal conductivity measurements and an examination of the mechanical properties after 28 days of curing.

1. Introduction:

The urgent environmental challenge confronting humanity is underscored by the prominent role of the buildings sector, accounting for a significant portion of the world's climate-altering emissions. This industry plays a significant role, influencing both power usage and the release of carbon dioxide [1]. The substantial emissions from energy consumption in buildings [2–6], encompassing heating, cooling, lighting, and appliance power, emphasize the need for innovative solutions [7,8]. The integration of recycled waste as a novel technology presents a promising avenue for innovating in architecture with minimal environmental impact, all while maintaining optimal thermal comfort in buildings [9]. Various waste materials are employed to enhance the physical characteristics of cement-based materials. One of the prominent wastes that are disposed to the industrial wastes chains is textile [10,11], that has been studied throughout the years as a reinforcement in construction components [12–14]. Where Rubino et al. [15] examined the thermal attributes demonstrated that the materials under scrutiny could effectively rival conventional insulators, displaying a thermal conductivity of less than 0.05 W/(m·K). This includes the utilization of natural filaments [16] sourced from renewable natural reservoirs, such as flax [17], and other fibers emitted from vegetal sources [18,19]. Animal fibers, including unconventional sources like human hair [20], serve as reinforcing materials. Research indicates that the incorporation of protein-based fibers enhances the strength of construction materials. Kanagalakhmi et al. [21] studied the integration of hair strands in 0.5, 1 and 1.5 by weight of the cement material, led to a general improvement in the compressive strength of the concrete, ranging from 1% to 12%. Additionally, there was an increase of up to 5% in the flexural strength of the concrete test specimens. The thermal insulation is evaluated as the waste percentage increases, revealing that a higher proportion of waste results in increased insulation properties for the material. In our research, we employed two distinct types of waste: mortars integrating natural fibers from human hair (MHF) and mortars incorporating textile fibers (MTF). The mortar formulation involved substituting sand volume with percentages ranging from 10% to 50%. These composite materials were then subjected to thorough thermal and mechanical characterization.

ISSN: 1737-9334

2. Materials:

The components employed in crafting the cement-based samples include Portland cement CEM II 32.5 N and natural sand AF-R-0/2-S, aligning with the specifications outlined in the European standard EN-197-1:2011 [22]. Two varieties of fibers were utilized in the integration of the mortars. The first type consists of mortars incorporated with textile fibers (MTF) predominantly composed of linen, polyester, and cotton fibers, sourced from the textile manufacturing industry [23]. The second fiber type comprises natural filaments derived from human hair (MHF), consisting of 95% keratin, a helical fibrous (propeller-shaped) protein [24]. These fibers were sourced from waste collected at hairdressing salons. Mortars with reinforcement were created by substituting the volume fractions of sand with 10%, 20%, 30%, 40%, and 50% of either of the two types of fibers.

3. Preparation:

Initially, the materials were blended in a dry state, followed by manual mixing with the waste fibers after their immersion in water. Subsequently, the remaining water was introduced. All mixtures were prepared using a mechanical mixer in accordance with European standards terminology [25]. Following that, the prepared mixture will be poured into molds and allowed to dry for 24 hours in a climatic chamber set at a temperature of 20°C. The concluding step involves placing the samples, extracted from the molds, into a water tank for a curing period of 28 days, after this period the samples will be extracted from the water and ready for the different characterization tests as shown in Fig. 1.

(a) (b)

Fig. 1: (a) Textile reinforced mortars, (b) Hair-reinforced mortars after 28 days of curing.

4. Characterization tests:

The cured bulk density was examined following the European standard EN 1015-10. The samples were placed under a temperature of 60 °C in a oven to dry until a content mass is attained [26]. To characterize the properties of the hardened cementitious composites, flexural and compressive strength tests were conducted using the EZ50 apparatus presented in Fig. 2(b) in conformity with EN standards [27]. The heat transfer of the samples was determined using the Hot Disk TPS 500, illustrated in Fig. 2(a) within a climatic chamber set at a temperature of 20 °C, following the guidelines outlined in ISO-22007-2 standard [28].

ISSN: 1737-9334

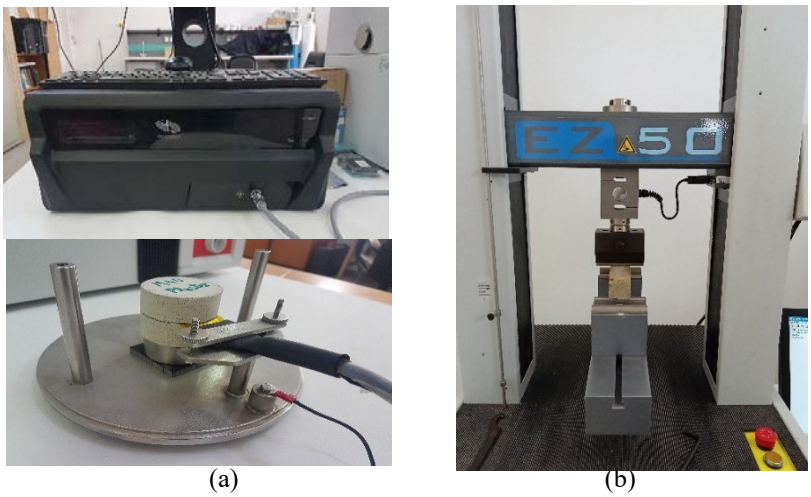

(a) (b)

Fig. 2: Thermal and mechanical testing materials (a) Hot Disk apparttus, (b) EZ50 testing machine.

5. Results and discussion:

Physical properties:

The variation in bulk density of the composites in terms of the proportion of reinforcing materials is illustrated in Fig. 3, the graph demonstrates that plain mortar has a higher apparent density, reaching a value of 2027 kg/m^3. The incorporation of both fiber types in mortar reduced the density, however the hair-reinforced composites have higher bulk density values than MTF. The lowest value was recorded at MTF for the 50% of waste addition at 1269 kg/m^3, the same results were found with Demircan et al. [29] where mortars integrated with animal fibers had higher values of dry bulk density than those of synthetic fibers.

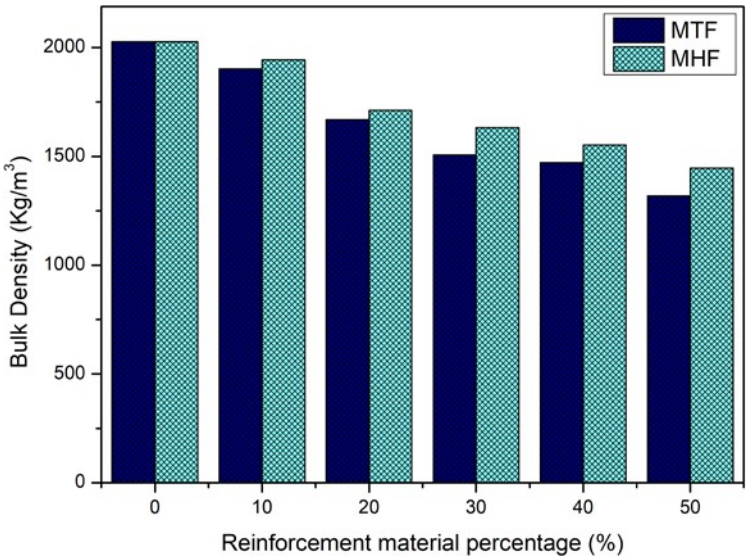

Fig. 3: Bulk density of the two types of mortars after 28 days of curing.

Mechanical tests:

In Fig. 4(a), the flexural strength was observed to decrease as waste fiber content increased, reaching a decrease of about 53% and 58% for both MTF50 and MHF50 respectively, when compared to the plain mortar.

ISSN: 1737-9334

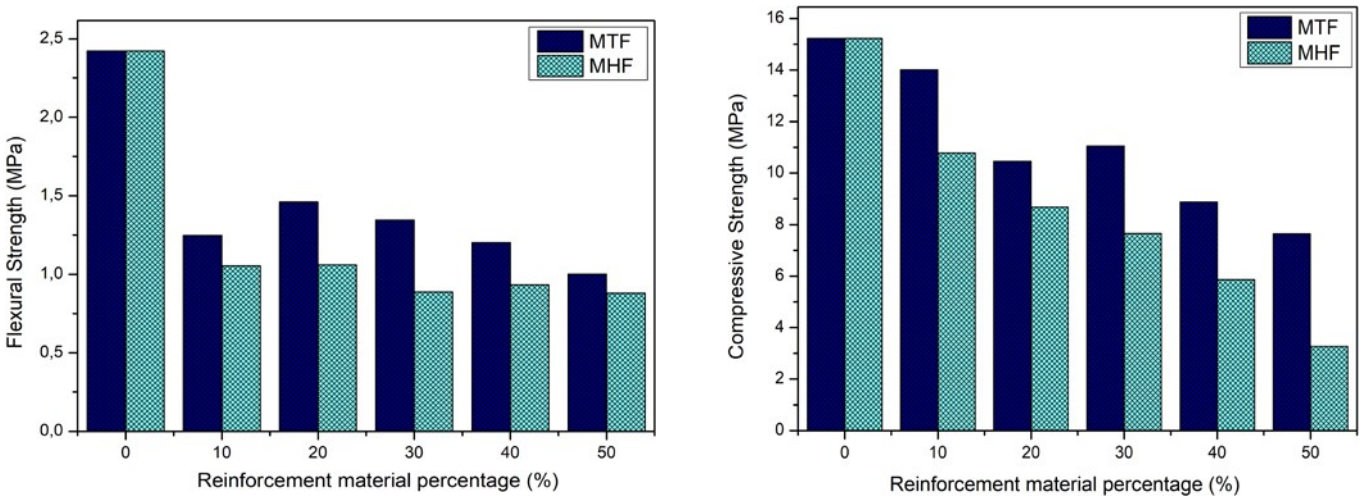

(a) (b)

Fig. 4: Mechanical test results of the samples after 28 days of curing: (a) Flexural strength, (b) Compressive strength.

The findings for the compressive strength are illustrated in Fig. 4(b). The MTF samples exhibited higher compressive strength than MHF samples after 28 days of curing, recording the lowest value at 3.27 MPa for a 50% of integration of hair which violates the rules to be respected for European standard EN 998-1 [30] in order for this composite to be considered as a coating material in buildings.

5.3 Thermal conductivity:

The Fig. 5 presents the thermal conductivity of the MHF and MTF composites. Increasing reinforcing material reduced thermal conductivity regardless of fiber type. Regarding the 28-day thermal conductivity, both textile types show a similar result, reaching values of 0.72 W/mK and 0.91 W/mK for MTF50 and MHF50 samples respectively.

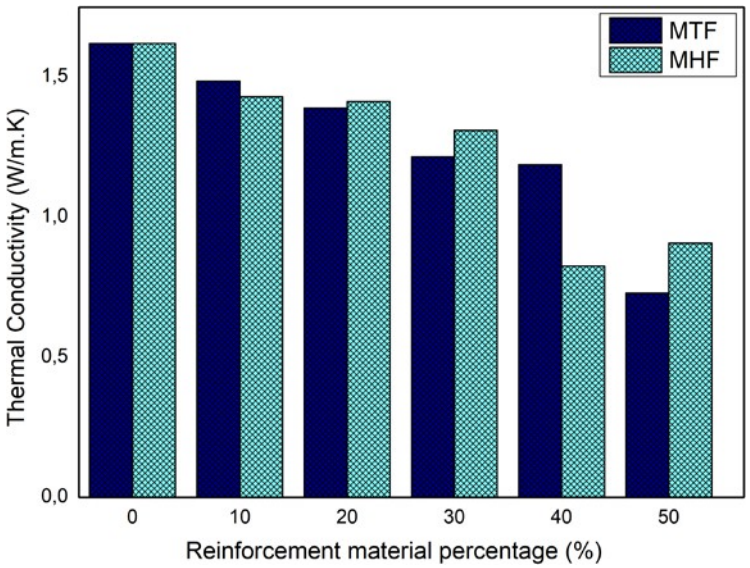

Fig. 5: Thermal conductivity of MTF and MHF samples after 28 days of curing.

6. Conclusion:

In order to mitigate the adverse environmental impact of advanced materials, achieving complete degradation is essential yet challenging. In light of this, our findings suggest that composites reinforced with a substitution percentage below 50% for the studied textile and natural fibers can

ISSN: 1737-9334

effectively meet thermal insulation objectives without compromising the required mechanical resistance standards.

Reference:

[1] UNEP, "2021 Global Status Report for Buildings and Construction: Towards a Zero-emission," *Effic. Resilient Build. Constr. Sect.*, pp. 1–105, 2021.

[2] S. Bouadila, S. Skouri, S. Kooli, M. Lazaar, and A. Farhat, "Experimental study of two insulated solar greenhouses one of them use a solar air heater with latent heat," 2015. doi: 10.1109/IREC.2015.7110873.

[3] S. Bouadil, S. Skouri, S. Kooli, M. Lazaar, and A. Farhat, "Solar energy storage application in Tunisian greenhouse by means of phase change materials," *2014 Int. Conf. Compos. Mater. Renew. Energy Appl. ICCMREA 2014*, pp. 0–3, 2014, doi: 10.1109/ICCMREA.2014.6843795.

[4] R. Ayed, S. Baddadi, S. Bouadila, S. Skouri, and M. Lazaar, *Architectural Development of the Buildings' Envelope to Improve Energy Efficiency*. Springer International Publishing, 2022. doi: 10.1007/978-3-031-00808-5_105.

[5] S. Bouadila, S. Baddadi, S. Skouri, and R. Ayed, "Assessing heating and cooling needs of hydroponic sheltered system in mediterranean climate: A case study sustainable fodder production," *Energy*, vol. 261, no. PB, p. 125274, 2022, doi: 10.1016/j.energy.2022.125274.

[6] S. Bouadila, S. Baddadi, T. ur Rehman, and R. Ayed, "Experimental investigation on the thermal appraisal of heat pipe-evacuated tube collector-based water heating system integrated with PCM," *Renew. Energy*, vol. 199, no. August, pp. 382–394, 2022, doi: 10.1016/j.renene.2022.09.004.

[7] A. Dellagi, R. Ayed, S. Bouadila, and A. Guizani, "Study of the thermal behavior of a heated brick containing a phase change material," *2022 13th Int. Renew. Energy Congr. IREC 2022*, vol. 1, no. Irec, pp. 5–9, 2022, doi: 10.1109/IREC56325.2022.10002002.

[8] R. Ayed, S. Baddadi, A. Dellagi, S. Bouadila, and M. Lazaar, "Thermal behavior improvement of building materials using expanded polystyrene," *2022 13th Int. Renew. Energy Congr. IREC 2022*, no. Irec, pp. 13–16, 2022, doi: 10.1109/IREC56325.2022.10002016.

[9] M. R. Gehlot and S. Shrivastava, "'Solid industrial waste generation and its valorization in developing sustainable building materials- A state of the art review,'" *Mater. Today Proc.*, no. xxxx, 2023, doi: 10.1016/j.matpr.2023.07.134.

[10] R. Ayed, S. Bouadila, S. Skouri, L. Boquera, L. F. Cabeza, and M. Lazaar, "Recycling Textile Waste to Enhance Building Thermal Insulation and Reduce Carbon Emissions: Experimentation and Model-Based Dynamic Assessment," *Buildings*, vol. 13, no. 2, 2023, doi: 10.3390/buildings13020535.

[11] A. Ahmed, A. Qayoum, and F. Q. Mir, "Spectroscopic studies of renewable insulation materials for energy saving in building sector," *J. Build. Eng.*, vol. 44, no. March 2020, p. 103300, 2021, doi: 10.1016/j.jobe.2021.103300.

[12] R. Ayed, A. Dellagi, S. Skouri, S. Baddadi, S. Bouadila, and M. Lazaar, "Sustainable insulation solutions for hydroponic greenhouses: The effects of textile waste reinforcement on thermal microclimate," *J. Build. Eng.*, vol. 73, p. 106710, 2023, doi: 10.1016/j.jobe.2023.106710.

[13] R. Ayed, E. Borri, G. Gasa, S. Bouadila, and L. F. Cabeza, *An Experimental Study on the Thermo-mechanical Properties of Cement Mortar with Textile Fibers for Building Applications*, vol. 43. 2023. doi: 10.1007/978-3-031-33211-1_103.

[14] L. N. Koutas and C. G. Papakonstantinou, "Flexural strengthening of RC beams with textile-reinforced mortar composites focusing on the influence of the mortar type," *Eng. Struct.*, vol. 246, no. July, p. 113060, 2021, doi: 10.1016/j.engstruct.2021.113060.

[15] C. Rubino, S. Liuzzi, P. Stefanizzi, and F. Martellotta, "Characterization of sustainable building materials obtained from textile waste : From laboratory prototypes to real-world manufacturing processes," *J. Clean. Prod.*, vol. 390, no. July 2022, p. 136098, 2023, doi: 10.1016/j.jclepro.2023.136098.

[16] D. Jiang *et al.*, "Effect of thermal insulation components on physical and mechanical properties of plant fibre composite thermal insulation mortar," *J. Mater. Res. Technol.*, vol. 9, no. 6, pp. 12996–13013, 2020, doi:

ISSN: 1737-9334

10.1016/j.jmrt.2020.09.009.

[17] P. Sadrolodabaee, J. Claramunt, M. Ardanuy, and A. de la Fuente, "Characterization of a textile waste nonwoven fabric reinforced cement composite for non-structural building components," *Constr. Build. Mater.*, vol. 276, p. 122179, Mar. 2021, doi: 10.1016/J.CONBUILDMAT.2020.122179.

[18] L. Tang, T. Liu, P. Sun, Y. Wang, and G. Liu, "Sisal fiber modified construction waste recycled brick as building material : Properties , performance and applications," *Structures*, vol. 46, no. November, pp. 927–935, 2022, doi: 10.1016/j.istruc.2022.10.126.

[19] M. Zakaria, M. Ahmed, M. Hoque, and S. Islam, "Scope of using jute fiber for the reinforcement of concrete material," *Text. Cloth. Sustain.*, 2016, doi: 10.1186/s40689-016-0022-5.

[20] N. Bheel, P. Awoyera, O. Aluko, S. Mahro, A. Viloria, and C. A. S. Sierra, "Sustainable composite development: Novel use of human hair as fiber in concrete," *Case Stud. Constr. Mater.*, vol. 13, p. e00412, 2020, doi: 10.1016/j.cscm.2020.e00412.

[21] A. S. Kanagalakhmi, B. Indhuja, U. Rithisri, and R. P. K. Devi, "Study on Human Hair in Concrete As a Fiber Reinforcement," vol. 8, no. 4, pp. 173–181, 2021.

[22] EN 197-1, "EN 197-1," Dec. 1992

[23] A. Tilioua, L. Libessart, and S. Lassue, "Characterization of the thermal properties of fi brous insulation materials made from recycled textile fi bers for building applications : Theoretical and experimental analyses," *Appl. Therm. Eng.*, vol. 142, no. August 2017, pp. 56–67, 2018, doi: 10.1016/j.applthermaleng.2018.06.071.

[24] A. Gupta, "Human Hair '" Waste "' and Its Utilization : Gaps and Possibilities," vol. 2014, 2014.

[25] EN 1015-2, "Methods of testing mortars for masonry - Part 2: bulk sampling of mortars and preparation of mortars for testing," 1999.

[26] EN 1015-10, "Methods of test for mortar for masonry - Part 10: Determination of dry bulk density of hardened mortar".

[27] EN 1015-11, "Methods of test for mortar for masonry - Part 11: Determination of flexural and compressive strength of hardened mortar," 2020

[28] ISO 22007-2, "Plastics - Determination of thermal conductivity and thermal diffusivity - Part 2: Transient plane heat source (hot disc) method," *Annu. B. ofASTM Stand.*, vol. 2008, p. 17, 2008.

[29] R. K. Demircan, B. A. Tayeh, D. N. Celik, G. Kaplan, and D. E. Tobbala, "The effect of animal and synthetic fibers on the physico-mechanical durability and microstructure properties of natural hydraulic lime-based mortars," *Mater. Today Commun.*, vol. 35, no. March, p. 106041, 2023, doi: 10.1016/j.mtcomm.2023.106041.

[30] EN 998-1:2017, "Specification for mortar for masonry - Part 1: Rendering and plastering mortar," 2005.

Comparative analysis of temperature variations inside a vertical greenhouse heated with latent and sensitive heating systems

Dorra cherif [*,1], Rabeb Ayed [1], Salwa Bouadila [1] and AmenAllah Guizani [1]

[1] *Centre de Recherches et des Technologies de l'Energie, Thermal Processes Laboratory Technopole de Borj-Cédria, BP: 95, Hammam Lif, Ben Arous, Tunisia*

Email 1 - cherifdorra11@gmail.com
Email 2 - amenallah.guizani@crten.mesrs.tn
Email 3 - salwa.bouadila@crten.rnrt.tn

Abstract

This study focuses on the energy-intensive nature of the heating process in agricultural greenhouses during cold periods. To improve energy efficiency, two different heating systems were integrated into a hydroponic greenhouse. The first is a novel dual solar air collector with latent heat storage (SAC-2 beds), while the second is a solar water heater system (SWHS) with two vacuum tube collectors for sensitive heat storage. The results show that SAC-2 beds contribute to higher nighttime temperatures and the solar water system achieves the highest daytime temperatures. Without a heating system, the greenhouse will experience significant temperature fluctuations, which can be up to 12°C between different levels. The implemented heating system improves thermal stratification with higher temperatures in the upper greenhouse levels.

Keyword: Hydroponic greenhouse, Microclimate optimization, Solar collectors, Phase change materials.

1. Introduction

The heating process during cold periods represent the most energy-intensive process in the entire agricultural greenhouse operation. Therefore, the use of solar energy and its storage in the form of latent heat to improve the energy efficiency of the greenhouse microclimate can only bring positive results. In this context, several researches studied the effect of exploring solar energy on the energy consumption and the microclimate of greenhouses. The research by Liu et al. [1] focuses on a greenhouse that requires additional heat at night to maintain an air temperature above 20 °C. They implement an innovative wall panels made from a phase change composite material. Benli and Durmus [2] developed a geothermal heat pump system

ISSN: 1737-9334

with latent heat storage to adjust the air temperature in the greenhouse. In a winter scenario, Bouadila et al. [3]–[5] installed an air solar collector with a latent storage collector in a chapel-shaped greenhouse with an area of 14.8 m^2. The results showed that the developed system increased the greenhouse temperature by 5°C and reduced the relative humidity by up to 17%. The air solar collector provided 30% of the total nighttime heating demand, with stored heat accounting for approximately 56% of the total excess daytime heat in the greenhouse. To remedy the stratification problem, several climate regulation tools are available. Among these systems are shading techniques [6], [7] and evaporative cooling in summer, dehumidification in winter and ventilation techniques (natural and forced) [8], [9]. In this context, Revathi et al. [10] developed a solar-powered forced ventilation system that emphasized energy saving and ensuring thermal comfort in the greenhouse.

In pursuit of energetic optimization of the microclimate, this research investigated two heating systems that were integrated, designed and implemented taking into account the specific energy needs of the hydroponic environment. The first is an innovative double bed solar air collector with latent heat storage (SAC-2 beds). The second is a solar water heater system (SWHS) with two vacuum tube collectors.

2. Description of the experimental device

2.1 Description of SAC-2 beds

Designed for greenhouse heating, the SAC-2 beds solar collector (Fig. 1) differs from traditional collectors in that it replaces the flat absorber with a set of black nodules containing a phase change material that can operate even in low sunlight. It consists of two layers, each consisting of 156 spherical nodules. These nodules contain CRISTOPIA brand phase change materials and form the absorber of the collector. The 312 nodules are arranged on two metal grids, each with twelve columns and thirteen lines. These two beds are stacked in a square box with a dimension of 1.05 m and a volume of 0.28 m^3 and are mounted on a metal support facing due south and forming an angle of inclination of 30° from the horizontal. Above the box is a converging piece of aluminum sheet that connects the collector to the greenhouse. To ensure the greenhouse effect and minimize convective and radiant heat losses from the absorber, the collector is covered by a transparent cover glass with an area of 1 m^2 and a thickness of 0.004 m. There are also two openings in the design of the SAC-2 beds, an opening below the collector allows cold air to enter and a second opening at the top in the upper part of the convergent allows hot air to exit from the collector to the greenhouse. The exchange between the incoming air and the absorber inside the collector is ensured by an air extractor controlled by a speed controller. These openings change position according to the operating mode of the SAC-2 beds collector; They open when charging and close when discharging. To ensure thermal insulation of the collector, a 5 cm thick layer of Arma Flex covers the converging side and rear surfaces of the collector. This insulation resists heat and moisture, is flexible and quick and easy to use. The nodules forming the absorber have a spherical shape made by extrusion blow molding and whose caps are welded by ultrasound, taking into account the phenomenon of expansion to avoid the constraints of the shell. They are made from a blend of polyolefins that ensure chemical neutrality to heat transfer fluids

ISSN: 1737-9334

and phase change materials. These nodules contain calcium chloride hexahydrate as a phase change material.

Fig. 1. Double bed solar air collector with latent thermal storage (SAC-2 beds).

2.2. Description of the SWHS system

The second experience considers the use of a heating system (SWHS) consisting mainly of solar-water collectors for heating the hydroponic greenhouse. The main idea heating the climate of the hydroponic greenhouse while homogenizing the temperature and reducing thermal stratification between the different levels of the culture trays. For this reason, the principle of this system is to provide the same heat to the different levels of the greenhouse through a multi-stage heat exchanger arranged under the culture dishes at different vertical levels [11]. The water heating is guaranteed by the two vacuum collectors shown in the Fig. 2 [12]. During the daytime, the absorber tubes capture the solar energy and the heat exchanger transfers it to the heat transfer fluid in the form of thermal energy. The water heated by the collectors is then stored in the tank until it is needed. As soon as the circuit starts operating, the pump delivers the stored hot water to the water collector and from there to the coils to circulate it among all the culture dishes. After passing through the multi-stage heat exchanger, the water is collected in the second collector, sucked in and sent back to the tank, where it compensates for the extracted thermal energy and reaches further degrees Celsius to do the same thing again. This means that the hot water leaves the storage tank at the same temperature and circulates in the multi-stage heat exchanger, producing almost the same amount of heat.

Fig. 2. Evacuated tube solar collectors used in the SWHS.

3. Results

Fig. 3 shows the temperature inside the hydroponic greenhouse before heating and after heating using the SAC-2 beds and the SWHS system. For this experience, we selected three days with comparable climatic conditions. We note that the lowest temperature corresponds to

ISSN: 1737-9334

the case of the greenhouse without heating. For heating with the SWHS, it is characterized by the largest daytime temperature, which is explained by the sensitive storage during the day where the vacuum collectors provide the highest amount of heat to the water that subsequently goes circulate to heat the greenhouse. Regarding heating with the SAC-2 beds, it is characterized by the highest nighttime temperature, which is explained by the heat released by the latent thermal storage collector during the evening and evacuated into the hydroponic greenhouse.

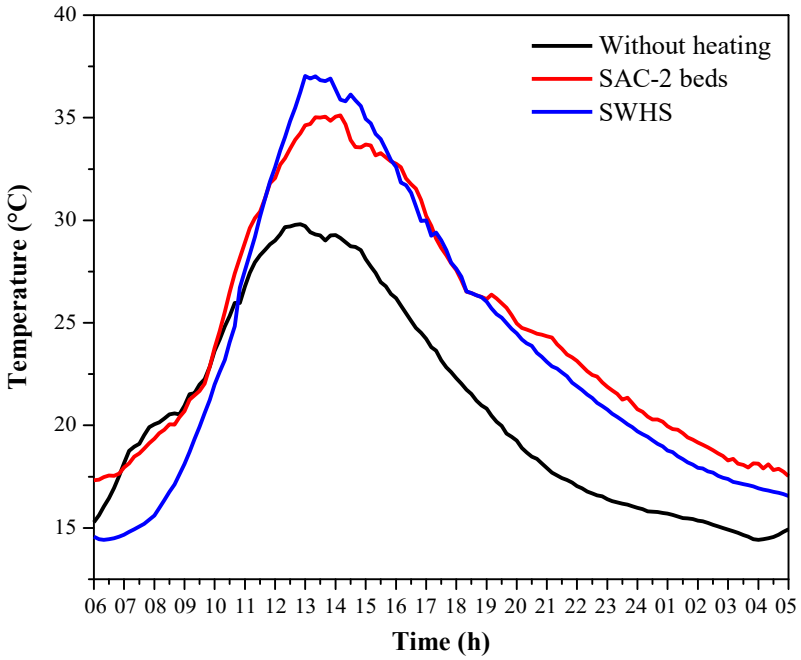

Fig. 3. Comparison of the temperature inside the hydroponic greenhouse before heating and after heating by SAC-2 beds and SWHS system.

4. Conclusion

This work presented a comparative study of the thermal behavior of a hydroponic greenhouse heated by two different heating systems. The first is a double bed solar air collector with latent heat storage (SAC-2 beds). The second is a solar water heater system (SWHS) with two vacuum tube collectors. The recorded experimental measurements showed that the temperature in the greenhouse varies significantly without a heating system, with a difference of up to 12 °C between different levels. However, the use of the heating system increases thermal stratification between the different levels, with temperatures being higher in the upper levels of the greenhouse. In fact, the SAC-2 beds is characterized by a higher nighttime temperature, while the heating with the solar water system has the highest daytime temperatures.

Acknowledgments

This study was supported by the Thermal Processes Laboratory of the Research and Technology Center of Energy (CRTEn) in Tunisia.

References

[1] Y. Liu, C. Chen, H. Yue, and G. Hailin, “An Application of Phase Change Technology

ISSN: 1737-9334

in a Greenhouse," *Envel. Technol. Build. Energy Effic.*, vol. 2, p. 2.5, 2006.

[2] H. Benli and A. Durmuş, "Evaluation of ground-source heat pump combined latent heat storage system performance in greenhouse heating," *Energy Build.*, vol. 41, no. 2, pp. 220–228, 2009.

[3] S. Bouadila, S. Kooli, S. Skouri, M. Lazaar, and A. Farhat, "Improvement of the greenhouse climate using a solar air heater with latent storage energy," *Energy*, vol. 64, 2014.

[4] S. Bouadil, S. Skouri, S. Kooli, M. Lazaar, and A. Farhat, "Solar energy storage application in Tunisian greenhouse by means of phase change materials," *2014 Int. Conf. Compos. Mater. Renew. Energy Appl. ICCMREA 2014*, pp. 0–3, 2014.

[5] S. Bouadila, S. Skouri, S. Kooli, M. Lazaar, and A. Farhat, "Experimental study of two insulated solar greenhouses one of them use a solar air heater with latent heat," in *2015 6th International Renewable Energy Congress, IREC 2015*, 2015.

[6] A. Senhaji, M. Mouqallid, and H. Majdoubi, "CFD Assisted Study of Multi-Chapels Greenhouse Vents Openings Effect on Inside Airflow Circulation and Microclimate Patterns," pp. 119–139, 2019.

[7] R. Ayed, A. Dellagi, S. Skouri, S. Baddadi, and S. Bouadila, "Sustainable insulation solutions for hydroponic greenhouses : The effects of textile waste reinforcement on thermal microclimate," *J. Build. Eng.*, vol. 73, no. February, p. 106710, 2023.

[8] D. Cherif and S. Bouadila, "Enhancing Crop Yield in Hydroponic Greenhouses : Integrating Latent Heat Storage and Forced Ventilation Systems for Improved Thermal Stratification (Under Review)," *Therm. Sci. Eng. Prog.*, vol. TSEP-D-23-, no. May, p. 102163, 2023.

[9] M. Muñoz, J. L. Guzmán, J. A. Sánchez, F. Rodríguez, and M. Torres, "Greenhouse Models as a Service (GMaaS) for Simulation and Control," *IFAC-PapersOnLine*, vol. 52, no. 30, pp. 190–195, 2019.

[10] S. Revathi, N. Sivakumaran, and T. K. Radhakrishnan, "Design of solar-powered forced ventilation system and energy-efficient thermal comfort operation of greenhouse," *Mater. Today Proc.*, vol. 46, pp. 9893–9900, 2019.

[11] S. Bouadila, S. Baddadi, S. Skouri, and R. Ayed, "Assessing heating and cooling needs of hydroponic sheltered system in mediterranean climate: A case study sustainable fodder production," *Energy*, vol. 261, p. 125274, Dec. 2022.

[12] S. Bouadila, S. Baddadi, T.- Rehman, and R. Ayed, "Experimental investigation on the thermal appraisal of heat pipe-evacuated tube collector-based water heating system integrated with PCM," *Renew. Energy*, Sep. 2022.

ISSN: 1737-9334

Evaluation of the Thermal Behavior of a Greenhouse with Reinforced Envelope

Rabeb Ayed[*,1], Sara Baddadi[1], Safa skouri[1], Salwa bouadila[1], Mariem Lazaar[1]

[1] *Centre de Recherches et des Technologies de l'Energie, Thermal Processes Laboratory Technopole de Borj-Cédria, BP: 95, Hammam Lif, Ben Arous, Tunisia*

* *Corresponding author:ayedrabeb09@gmail.com*

Abstract

Repurposing waste into building materials offers a dual solution to energy shortages and environmental pollution. This study investigates the incorporation of textile fiber wastes into concrete blocks to improve the microclimate of agricultural shelters. A year-long experiment compared a transparent greenhouse (Ref_Gh) and an hydroponic greenhouse thermally insulated with thermal panels (THP_Gh). Using cement blocks with 30% textile fiber replacement, a hydroponic greenhouse (TRC_Gh) was evaluated using a numerical model. TRC_Gh showed a higher diurnal temperature variation than THP_Gh, but remained significantly lower than Ref_Gh. The study concludes that a hydroponic greenhouse with textile-reinforced cement blocks provides enhanced thermal performance compared to plexiglass structures. However, greenhouses with thermal panels still outperform in thermal efficiency. This research highlights the benefits of recycling textiles for building insulation and presents an innovative and environmentally friendly strategy to improve the microclimate of hydroponic greenhouses.

Keywords: Thermal insulation, Agricultural greenhouse, Textile fibers, Thermodynamic model**.**

1. Introduction

Agricultural production in greenhouses is considered a promising alternative to outdoor cultivation [1]. While greenhouses provide controlled environments for optimal plant growth and nutrition [2], they can be expensive and energy intensive [3][4]. Accordingly, the use of energy in agricultural shelters needs to be addressed by adoptingnew sustainable methods[5]–[7].Energy consumption varies depending on various parameters, particularly the integration of thermal insulation [8][9]. Many researchers have studied the influence of thermal insulation on greenhouses. For example, one study examined the thermal performance of a tunnel greenhouse with double glazing made from polycarbonate panels [10], while another examined the thermal environment of three greenhouses with different north wall designs and found that reinforced walls performed better than hollow block walls [11]. In this context, it is imperative to advance the

ISSN: 1737-9334

development of new, extremely cost-effective insulation materials for shelterscover [12]–[16]. This is particularly important due to the integration of reinforcing materials into a cement matrix, for example in the form of concrete.In this regard, this study focuses on evaluating the possibility of using post-industrial textile waste to reinforce cement blocks to improve the thermal performance of greenhouses. A comparative study was carried out to analyze the thermal behavior of three types of greenhouses.

2. Studied greenhouses

This research showed both experimental and numerical analyzes to evaluate and compare the thermal performance of three types of agricultural shelters (Fig. 1). Two greenhouses were built on the Mediterranean coast in northern Tunisia: a reference greenhouse (Ref_Gh) with a Plexiglas cover and a hydroponic greenhouse (THP_Gh) with thermal panels. The experimental measurements of the thermal performance in the two agricultural greenhouses (Ref_Gh and THP_Gh) were conducted in 2021. Various sensors were used, including K-type thermocouples, pyranometers, pyrheliometers, HMP155A and an ultrasonic wind sensor. Climate parameters were recorded every 10 minutes via a Campbell CR5000 data acquisition system, providing detailed insights into greenhouse conditions. The third greenhouse (TRC_Gh) uses textile-reinforced concrete blocks in which 30% of the sand was replaced by textile fiber wastes and which had an equivalent thermal conductivity (U) of 1.88 W/m^{2}K. These textile-reinforced concrete blocks were integrated into a hydroponic greenhouse structure, reflecting the geometry of THP_Gh. The study established a thermodynamic MATLAB model to simulate air temperature fluctuations in different types of greenhouses, integrating their structural thermophysical properties. The climatic conditions from the experimental site were integrated to perform and validate simulations for Ref_Gh and THP_Gh shelters. The model was then used to simulate the thermal microclimate of the TRC_Gh greenhouse.

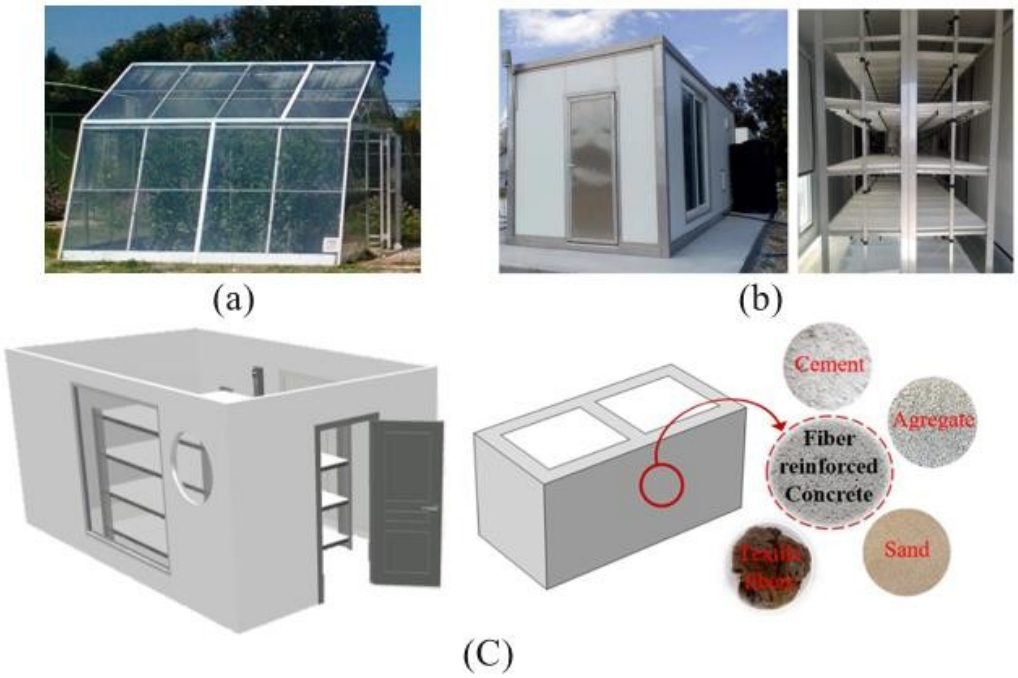

Fig. 1. Studied greenhouses (a) Ref_Gh, (b) THP_Gh and (c) TRC_Gh.

ISSN: 1737-9334

3. Results

3.1. Numerical model validation

The comparison between the results of the numerical model and the experimental data from the Ref_Gh and THP_Gh greenhouses is shown in Fig. 2. The graph shows a close agreement between predicted and experimentally recorded air temperature values in the reference and hydroponic greenhouses. Both Ref_Gh and THP_Gh showed temperature variations of 0.5 °C to 70 °C and 4 °C to 45.5 °C, respectively, with generally minor differences between predicted and experimental data. While occasional differences were noted, possibly due to infiltration in experimental setups and model assumptions, the overall agreement underscores the effectiveness of the model in accurately predicting air temperature variations across different greenhouse types.

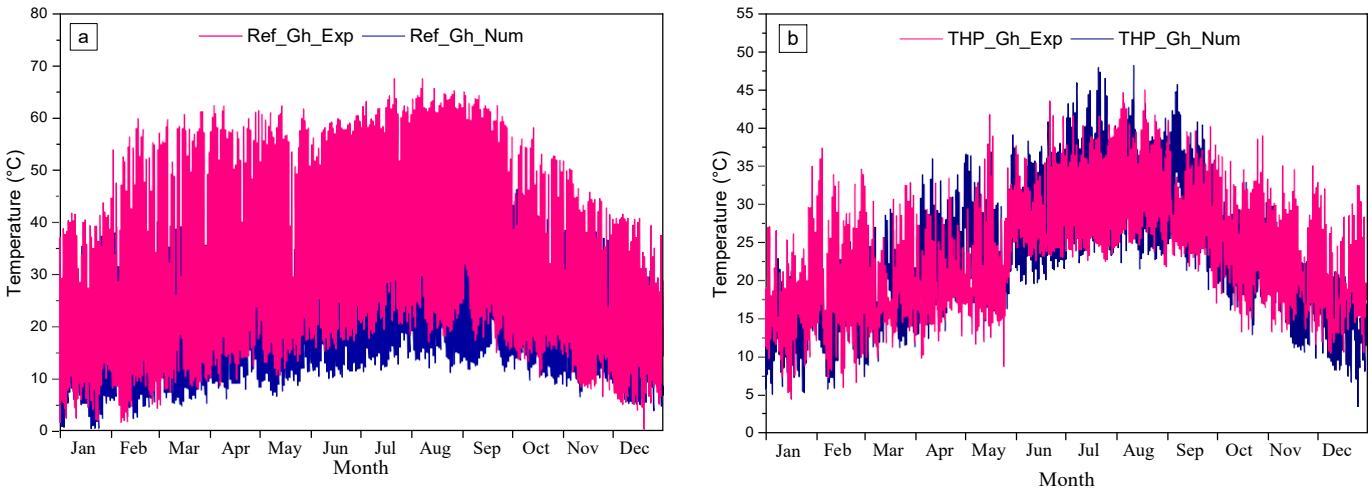

Fig. 2. Comparison between experimental and predicted temperature variations in (a) Ref_Gh and (b) THP_Gh greenhouses.

3.2. Microclimate assessment

After the validation, the model was used to determine the air temperature variation inside the textile reinforced greenhouse. Fig. 3show the temperature differences between the interior environment of each greenhouse and the exterior air temperature. For Ref_Gh, the average temperature difference was 11°C throughout the year. In the case of THP_Gh, the temperature difference varied between -7°C and 10°C. Likewise, the temperature difference for TRC_Gh mainly fluctuated between -7.8 °C and 9.9 °C. Accordingly, Ref_Gh has the highest energy exchange with the outside environment, resulting in inferior thermal performance compared to insulated greenhouses. Overall, both fiber insulation panels and thermal insulation panels prove to be effective insulation materials, with the selection between them depending on the specific necessitates and demands of the greenhouse and insulation application.

ISSN: 1737-9334

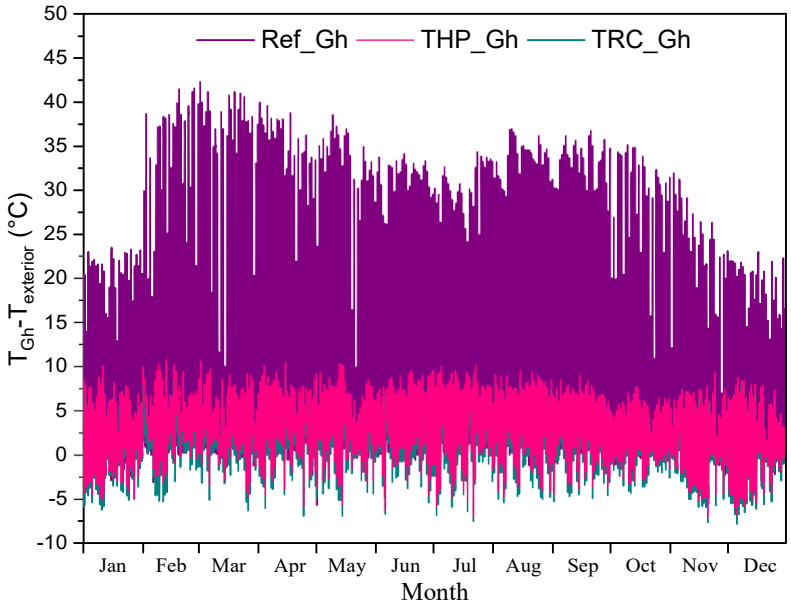

Fig. 3. Temperature difference between the exterior and interior temperature of each greenhouse.

4. Conclusion

The study investigates the performance of a greenhouse built withtextile-reinforced blocks. The temperature inside the textile-reinforced greenhouse was slightly higher than ina thermal panel greenhouse, but it still has a considerably lower temperature than a transparent greenhouse.

Acknowledgments

This study was supported by the Thermal Processes Laboratory of the Research and Technology Center of Energy (CRTEn) in Tunisia.

References

[1] N. Khammayom, N. Maruyama, C. Chaichana, and M. Hirota, “Impact of environmental factors on energy balance of greenhouse for strawberry cultivation,” *Case Stud. Therm. Eng.*, vol. 33, p. 101945, May 2022.

[2] H. M. Ljungqvist, L. Mattsson, M. Risberg, and M. Vesterlund, “Data center heated greenhouses, a matter for enhanced food self-sufficiency in sub-arctic regions,” *Energy*, vol. 215, p. 119169, Jan. 2021.

[3] C. A. O’Sullivan, G. D. Bonnett, C. L. McIntyre, Z. Hochman, and A. P. Wasson, “Strategies to improve the productivity, product diversity and profitability of urban agriculture,” *Agric. Syst.*, vol. 174, pp. 133–144, Aug. 2019.

[4] S. Bouadila, S. Baddadi, S. Skouri, and R. Ayed, “Assessing heating and cooling needs of hydroponic sheltered system in mediterranean climate: A case study sustainable fodder production,” *Energy*, vol. 261, p. 125274, Dec. 2022.

[5] S. Bouadil, S. Skouri, S. Kooli, M. Lazaar, and A. Farhat, “Solar energy storage application in Tunisian greenhouse by means of phase change materials,” *2014 Int. Conf. Compos. Mater. Renew. Energy Appl. ICCMREA 2014*, pp. 0–3, 2014.

ISSN: 1737-9334

[6] S. Bouadila, S. Skouri, S. Kooli, M. Lazaar, and A. Farhat, "Experimental study of two insulated solar greenhouses one of them use a solar air heater with latent heat," in *2015 6th International Renewable Energy Congress, IREC 2015*, 2015.

[7] S. Bouadila, S. Baddadi, T.- Rehman, and R. Ayed, "Experimental investigation on the thermal appraisal of heat pipe-evacuated tube collector-based water heating system integrated with PCM," *Renew. Energy*, Sep. 2022.

[8] V. F. Mendes, W. Fardin, R. R. Barreto, L. F. Caetano, and J. C. Mendes, "Sensitivity analysis of coating mortars according to their specific heat, specific gravity, thermal conductivity, and thickness in contribution to the global thermal performance of buildings," *Sustain. Mater. Technol.*, vol. 31, p. e00381, Apr. 2022.

[9] R. Ayed, A. Dellagi, S. Skouri, S. Baddadi, and S. Bouadila, "Sustainable insulation solutions for hydroponic greenhouses : The effects of textile waste reinforcement on thermal microclimate," *J. Build. Eng.*, vol. 73, no. February, p. 106710, 2023.

[10] E. Fabrizio, "Energy reduction measures in agricultural greenhouses heating: Envelope, systems and solar energy collection," *Energy Build.*, vol. 53, pp. 57–63, 2012.

[11] J. Wang, S. Li, S. Guo, C. Ma, J. Wang, and S. Jin, "Simulation and optimization of solar greenhouses in Northern Jiangsu Province of China," *Energy Build.*, vol. 78, pp. 143–152, 2014.

[12] R. Ayed, S. Baddadi, A. Dellagi, S. Bouadila, and M. Lazaar, "Thermal behavior improvement of building materials using expanded polystyrene," in *2022 13th International Renewable Energy Congress, IREC 2022*, 2022, no. Irec, pp. 13–16.

[13] A. Dellagi, R. Ayed, S. Bouadila, and A. Guizani, "Study of the thermal behavior of a heated brick containing a phase change material," in *2022 13th International Renewable Energy Congress, IREC 2022*, 2022, vol. 1, no. Irec.

[14] R. Ayed, S. Baddadi, S. Bouadila, S. Skouri, and M. Lazaar, "Architectural Development of the Buildings' Envelope to Improve Energy Efficiency," in *Advances in Science, Technology and Innovation*, Springer International Publishing, 2022, pp. 459–461.

[15] R. Ayed, S. Bouadila, S. Skouri, L. Boquera, and luisa F. Cabeza, "Recycling Textile Waste to Enhance Building Thermal Insulation and Reduce Carbon Emissions : Experimentation and Model-Based Dynamic Assessment," 2023.

[16] R. Ayed, E. Borri, G. Gasa, S. Bouadila, and L. F. Cabeza, "An Experimental Study on the Thermo-mechanical Properties of Cement Mortar with Textile Fibers for Building Applications," *RILEM Bookseries*, vol. 43, pp. 1153–1162, 2023.

ISSN: 1737-9334

A Networked Multi-Source Energy System Modelling and Stability Analysis

Gherbi Sofiane[*1], Aouati Ayoub[1], Ramazan Ayaz[2], and Sedraoui Moussa[3]

Badji Mokhtar Annaba University[1], Algeria, Yildiz Technical University[2], Turkey, 08 Mai 1945 Guelma University[3], Algeria

sofiane.gherbi@univ-annaba.dz
aouati.ayoub@univ-annaba.org
ayaz@yaldiz.edu.tr
msedraoui@gmail.com

Abstract. This article presents a novel design for a multi-source energy system utilizing the networked control system (NCS) paradigm. The primary objective is to investigate the feasibility of managing and distributing electrical energy among nearby producers/consumers, often referred to as "prosumers," through an existing communication network. To achieve this, an interconnected electric energy prosumer system with multiple nodes is established, featuring a centralized control and energy-sharing mechanism. Subsequently, a stability criterion, leveraging the Lyapunov-Krasovskii theorem, is introduced. This criterion incorporates a stochastic distributed network-induced delay model for each prosumer. It is formulated as a set of linear matrix inequalities (LMIs), the solution of which provides the maximum permissible upper limit for network-induced delay. Consequently, the assessment of these findings serves as a valuable tool, among others, in determining the maximum allowable separation distance between prosumers and making informed decisions regarding investment in a networked energy-sharing system.

Keywords: Multi-source energy, networked control system, Lyapunuv-Krasovskii stability.

1 Introduction

- The multi-sources energy systems are an active area of research and development nowadays, the development of such systems is expected to grow in the coming years as the demand for more efficient and sustainable energy solutions increases. These systems can integrate multiple energy sources including renewable energy, grid power, and stored energy [1]. It also enables efficient real-time energy sharing, management, and control between different prosumers through a communication network [2], in this context, several research works were published in recent years as [3-5]. Nevertheless, the network induced-delay which results from communication delay, packet dropouts, congestion..etc, can affect the stability of such systems [6-7]. In this, paper we present a stability analysis of a multisources networked energy system based on the Lyapunuv-Krasovskii stability theorem [8-9], with a stochastic delay distribution model, resulting in an LMI stability criterion, which after its resolution gives us the maximum allowable upper bound delay to keep the system stable, therefore, it can be considered as an important tool to support the decision to invest in an intelligent energy sharing system for close producers. This paper is organised as follow: section two presents the networked multi-source energy systems, with the state-space modeling. In the section 3, the stability analysis methodology is elaborated, focusing on the Lyapunov-Krasovskii theorem, with the the incorporation of a stochastic delay distribution model, and the derivation of the Linear Matrix Inequality (LMI) stability criterion. An application example is depicted in section four for a practical scenario within networked multi-source energy systems, where the obtained results are interpreted and discussed. Finally, a conclusion is given in section five, providing a summary of the proposed approach and the obtained results.

2 Networked Multı-Source Energy Systems Modelıng

The aim of this study is to establish a networked multi-source energy system from a microgrid. This system is designed

to facilitate energy collaboration and sharing among users, particularly in remote areas that are distant from the primary grid. The system's configuration can consist of various combinations of energy sources, energy storage facilities, and electrical loads. This paper specifically emphasizes a networked system based on multiple Solar Photovoltaic Energy Systems (SPVES) while considering non-uniformly distributed communication delays. However, it can be expanded to encompass additional energy sources.

2.1 SPVES State-Space Model

The solar photovoltaic energy system shown in Figure 1 consists of a PV array generator followed by a push-pull converter.

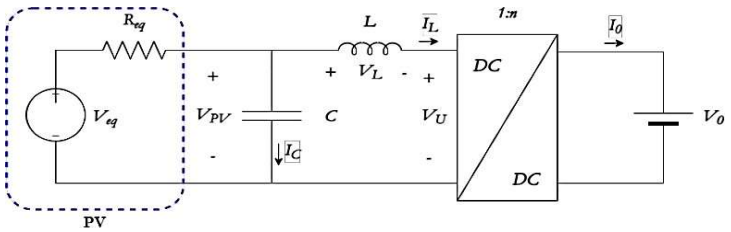

Fig. 1. SPVES with Push-Pull Converter [10]

This circuit is modeled as a small-signal representation. The state-space model of the entire system is provided by reference [10]:

$$\begin{bmatrix} \dot{\tilde{V}}_{PV} \\ \dot{\tilde{I}}_L \end{bmatrix} = \begin{bmatrix} -\frac{1}{R_{eq}C} & -\frac{1}{C} \\ \frac{1}{L} & 0 \end{bmatrix} \begin{bmatrix} \tilde{V}_{PV} \\ \tilde{I}_L \end{bmatrix} + \begin{bmatrix} 0 \\ -\frac{V_0}{Ln} \end{bmatrix} \tilde{d} \qquad (1)$$

$$y = \begin{bmatrix} 1 & 0 \end{bmatrix} \begin{bmatrix} \tilde{V}_{PV} \\ \tilde{I}_L \end{bmatrix}$$

where $\tilde{V}_{PV}$ is the capacitor voltage, $\tilde{I}_L$ is the inductor voltage and $\tilde{d}$ is the duty cycle (input control of the DC/DC converter).

The state matrix are: $A = \begin{bmatrix} -\frac{1}{R_{eq}C} & -\frac{1}{C} \\ \frac{1}{L} & 0 \end{bmatrix}, B = \begin{bmatrix} 0 \\ -\frac{V_0}{Ln} \end{bmatrix}$.

In addition, the adopted controller consists on a state feedback vector gain K.

3 Stability Analysis of the Networked Multı-Sources Energy Systems with Distributed Delay Approach

In a Networked Control System (NCS), the traditional control loop is integrated with a communication network, enabling the exchange of critical information among system components such as sensors, controllers, and actuators. This shared network serves as the medium for transmitting data including reference input, plant output, and control input. Figure 2 provides a typical graphical representation of the NCS structure, offering insights into the interactions and communication pathways among these components.

ISSN: 1737-9334

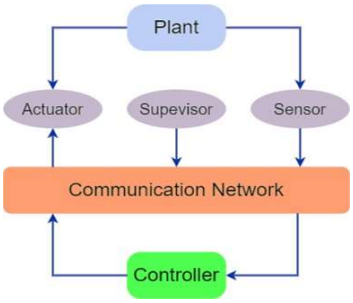

Fig. 2. Typical NCS structure

A significant aspect impacting NCS performance, especially in the context of Internet Protocol (IP) networks, is the non-uniform distribution of communication delays. We assume that the network-induced communication delay, denoted as $\tau(t)$, varies within the interval $[\tau_l, \tau_m]$, where τ_l represents the lower bound delay, τ_m signifies the maximum allowable delay bound (MADB), and τ_b is chosen within the interval range $[\tau_l, \tau_m]$. This variation in delays is principally observed in the lower interval $[\tau_l, \tau_b]$ [11-13]. Therefore, we can write:

$$\begin{cases} (1)\ \tau_l \leqslant \tau(t) \leqslant \tau_m < \infty, \quad \forall t \geqslant 0 \\ (2)\ \text{Prob}\left[\tau(t) \in [\tau_l, \tau_b)\right] = \bar{\delta} \\ \quad\ \text{Prob}\left[\tau(t) \in [\tau_b, \tau_m]\right] = 1-\bar{\delta} \end{cases} \tag{2}$$

where τ_b is a bound which get the probability of $\bar{\delta}$ for $[\tau_l, \tau_b)$.

Let define a stochastic variable $\delta(t)$ for further computation simplicity:

$$\delta(t) = \begin{cases} 1, & t : \tau(t) \in [\tau_l, \tau_b) \\ 0, & t : \tau(t) \in [\tau_b, \tau_m] \end{cases} \tag{3}$$

3.1 Stability Analysis

Now, considering a closed-loop control system with a communication delay that respects the probability law mentioned in Eq (1) as follows [14]:

$$\begin{cases} \dot{x}(t) = Ax(t) + \delta(t)BKx\left(t - \tau_l(t)\right) + (1-\delta(t))BKx\left(t - \tau_b(t)\right) \\ x(t) = \varrho(t), t \in [-\tau_m, -\tau_l] \end{cases} \tag{4}$$

where $x(t) \in \mathbb{R}^n$ and $u(t) \in \mathbb{R}^m$ are the state vector and control input vector, respectively. A and B are constant matrices with appropriate dimensions. K is the feedback gain of the network controller, $\varrho(t)$ is the initial condition function.

The following theorem is derived from Lyapunov-Krasovskii stability theorem (see [14] for more details)

Theorem

The system of Eq.(4) is asymptotically stable in the mean square, for given constants τ_l, τ_b, τ_m and matrix K, if there exist matrices $P > 0, Q_i > 0, R_i > 0, S_j > 0\ (i = 1,2,3,\ j = 1,2)$ with appropriate dimensions, such that the following LMIs holds:

$$\tilde{\Pi} = \begin{bmatrix} \Pi_{11} & \Pi_{12} & \Pi_{13} \\ * & \Pi_{22} & 0 \\ * & * & \Pi_{33} \end{bmatrix} < 0 \qquad (5)$$

where

$$\Pi_{11} = \begin{bmatrix} \Sigma_{11} & \Sigma_{12} & \Sigma_{13} & 0 & \Sigma_{15} & 0 \\ * & \Sigma_{22} & \Sigma_{23} & 0 & 0 & 0 \\ * & * & \Sigma_{33} & \Sigma_{34} & 0 & 0 \\ * & * & * & \Sigma_{44} & \Sigma_{45} & 0 \\ * & * & * & * & \Sigma_{55} & \Sigma_{56} \\ * & * & * & * & * & \Sigma_{66} \end{bmatrix}$$

$$\Pi_{12} = diag\left(A^{\mathrm{T}}, 0, \bar{\delta} K^{\mathrm{T}} B^{\mathrm{T}}, 0, (1-\bar{\delta}) K^{\mathrm{T}} B^{\mathrm{T}}, 0\right) Ones(6,5)\Xi$$

$$\Pi_{13} = \bar{\delta}(1-\bar{\delta}) diag\left(0, 0, K^{\mathrm{T}} B^{\mathrm{T}}, 0, -K^{\mathrm{T}} B^{\mathrm{T}}, 0\right) Ones(6,5)\Xi$$

$$\Pi_{22} = diag\left\{-R_1, -R_2, -R_3, -S_1, -S_2\right\},\ \Pi_{33} = \bar{\delta}(1-\bar{\delta})\Pi_{22}$$

$$\Xi = diag\left(\tau_l R_1, \tau_b R_2, \tau_m R_3, (\tau_b - \tau_l) S_1, (\tau_m - \tau_b) S_2\right)$$

and

$$\Sigma_{11} = PA + A^{\mathrm{T}} P + Q_1 + Q_2 + Q_3 - R_1 - R_2 - R_3, \Sigma_{12} = R_1$$

$$\Sigma_{13} = \bar{\delta} PBK + R_2, \Sigma_{15} = (1-\bar{\delta}) PBK + R_3 \Sigma_{22} = -Q_1 - R_1 - S_1$$

$$\Sigma_{23} = S_1, \Sigma_{33} = -2R_2 - 2S_1, \Sigma_{34} = R_2 + S_1, \Sigma_{44} = -Q_2 - R_2 - S_1 - S_2$$

$$\Sigma_{45} = S_2, \Sigma_{55} = -2R_3 - 2S_2, \Sigma_{56} = R_3 + S_2, \Sigma_{66} = -Q_3 - R_3 - S_2$$

$Ones(6,5)$ is an 6×5 matrix of ones.

4 Application, Results and Discussion

To illustrate the proposed approach, let's consider a networked energy system consisting of three promsumers having Solar Photovoltaic Energy Sources (SPVES) with the following numerical state space mumerical models:

Prosumer 1:

$$A = \begin{bmatrix} -\frac{5}{3}\times 10^3 & -\frac{5}{3}\times 10^4 \\ \frac{2}{3}\times 10^4 & 0 \end{bmatrix}$$

$$B = \begin{bmatrix} 0 \\ -\frac{35}{9}\times 10^5 \end{bmatrix}$$

$$K = [0.0006 \quad -0.00016]$$

Prosumer 2:

$$A = \begin{bmatrix} -\frac{4}{3}\times 10_3 & -\frac{4}{3}\times 10_4 \\ \frac{1}{3}\times 10^4 & 0 \end{bmatrix}$$

$$B = \begin{bmatrix} 0 \\ -\frac{30}{9}\times 10^5 \end{bmatrix}$$

$$K = [0.0005 \quad -0.00012]$$

ISSN: 1737-9334

Prosumer 3:

$$A = \begin{bmatrix} -\frac{7}{3} \times 10^3 & -\frac{7}{3} \times 10^4 \\ \frac{2}{3} \times 10^4 & 0 \end{bmatrix}$$

$$B = \begin{bmatrix} 0 \\ -\frac{40}{9} \times 10^5 \end{bmatrix}$$

$$K = [0.0007 \quad -0.0002]$$

Now, let's apply the theorem of section 3 in order to determine the maximum allowable communication delay bounds MADBs (bold) for different probabilities, that conseves the system stability for each prosumer. The following tables resumes the obtained results.

Table 1. MADBs for different probabilities (prosumer 1).

δ	*0.2*	*0.4*	*0.6*	0.8
$\tau(t) \in [10^{-6}\ 10^{-4}]$	$\mathbf{6.10^{-4}}$	$\mathbf{8.10^{-4}}$	$\mathbf{12.10^{-4}}$	$\mathbf{22.10^{-4}}$

Table 2. MADBs for different probabilities (prosumer 2).

δ	*0.2*	*0.4*	*0.6*	0.8
$\tau(t) \in [10^{-6}\ 10^{-4}]$	$\mathbf{8.10^{-4}}$	$\mathbf{11.10^{-4}}$	$\mathbf{17.10^{-4}}$	$\mathbf{33.10^{-4}}$

Table 3. MADBs for different probabilities (prosumer 3).

δ	*0.2*	*0.4*	*0.6*	0.8
$\tau(t) \in [10^{-6}\ 10^{-4}]$	$\mathbf{4.10^{-4}}$	$\mathbf{6.10^{-4}}$	$\mathbf{8.10^{-4}}$	$\mathbf{15.10^{-4}}$

4.1 Results Interpretation

From the preceding tables, if the probability of communication delay's $\tau(t)$ falls in the range $[10^{-6}\ 10^{-4}]$ is:

- 20% ($\delta = 0.2$), then the maximum allowable delay is 6.10^{-4} seconds for the first prosumer, 8.10^{-4} seconds for the second and 4.10^{-4} seconds for the third.
- 40% ($\delta = 0.4$), then the maximum allowable delay is 8.10^{-4} seconds for the first prosumer, 11.10^{-4}seconds for the second and 6.10^{-4} seconds for the third.
- 60% ($\delta = 0.6$), then the maximum allowable delay is 12.10^{-4} seconds for the first prosumer, 17.10^{-4} seconds for the second and 8.10^{-4} seconds for the third.
- 80% ($\delta = 0.8$), then the maximum allowable delay is 12.10^{-4} seconds for the first prosumer, 33.10^{-4} seconds for the second and 15.10^{-4} seconds for the third.

Based on the previous results, we can conclude that any multi-source energy system composed by the three prosumers from the previous example, must consider the maximum allowable communication delay for the stability of the entire system. This maximum delay should be determined as the minimum among the three prosumers based on the the différents probabilities.

5 Conclusion

This paper highlights the critical importance of managing communication delays in Networked Control Systems (NCSs) within multi-source energy systems context. It addresses a state space model from the non-uniform distribution of these delays and their probabilistic nature. After that, it conducts a stability analysis of such systems by determining the maximum allowable delays by rersolving an LMI Lyapunov-Krasovskii based stability criterion for differents probabilities. The results can serv as a decision-making tool for investment in such systems.

References

[1] P. Mancarella, "MES (multi-energy systems): An overview of concepts and evaluation models," Energy Vol. 65, 2014, pp. 1–17.
[2] M. Segatto et al, "14 - Telecommunication Technologies for Smart Grids: Total Cost Optimization," Advances in Renewable Energies and Power Technologies, Elsevier, 2018, pp 451-478, https://doi.org/10.1016/B978-0-12-813185-5.00007-3.
[3] Deng, Fang, et al. "Multisource energy harvesting system for a wireless sensor network node in the field environment." IEEE Internet of Things Journal 6.1 (2018): 918-927.
[4] Lee, Wai-Kong, et al. "Multi-source energy harvesting and storage for floating wireless sensor network nodes with long range communication capability." IEEE Transactions on Industry Applications 54.3 (2018): 2606-2615.
[5] Parmar, KP Singh, S. Majhi, and D. P. Kothari. "LFC of an interconnected power system with multi-source power generation in deregulated power environment." International Journal of Electrical Power & Energy Systems 57 (2014): 277-286.
[6] Tan, Cheng, Lin Li, and Huanshui Zhang. "Stabilization of networked control systems with both network-induced delay and packet dropout." Automatica 59 (2015): 194-199.
[7] Zhang, Wen-An, and Li Yu. "Modelling and control of networked control systems with both network-induced delay and packet-dropout." Automatica 44.12 (2008): 3206-3210.
[8] Kharitonov, Vladimir L., and Alexey P. Zhabko. "Lyapunov–Krasovskii approach to the robust stability analysis of time-delay systems." Automatica 39.1 (2003): 15-20.
[9] Zhenman, Gao, He Yong, and Wu Min. "New constructing method of Lyapunov-Krasovskii functionals for stability of time-varying delay systems." IECON 2017-43rd Annual Conference of the IEEE Industrial Electronics Society. IEEE, (2017).
[10] D. Fernandes, R. Almeida, T. Guedes, A. J. Sguarezi Filho, and F. Costa, "State feedback control for DC-photovoltaic systems," Electric Power Systems Research, vol. 143, pp. 794–801, Feb. (2017), doi:10.1016/j.epsr.2016.08.037
[11] Y. Tipsuwan, M.Y. Chow, Gain scheduling middleware: a methodology to enable existing controllers for networked control and teleoperation—part i: network control, IEEE Transactions on Industry Electronics 51 (6) (2004) 1218–1227.
[12] G.C. Walsh, H. Ye, L.G. Bushnell, Stability analysis of networked control systems, IEEE Transactions on Control Systems Technology 10 (2002) 438–446.
[13] H.C. Yan, X.H. Huang, M. Wang, Delay-dependent stability and stabilization criteria of networked control systems with multiple time-delays, Journal of Control Theory and Applications 4 (4) (2006) 321–326.
[14] Peng, Chen, et al. "A delay distribution based stability analysis and synthesis approach for networked control systems." Journal of the Franklin Institute 346.4 (2009): 349-365.

ISSN: 1737-9334

Experimental Analysis of a PV/Battery Hybrid Installation with Energy Storage

Safa Skouri[#1], Aymen Lachheb[*2] , Salwa Bouadila[#4]

[#] *Centre de Recherches et des Technologies de l'Energie, Thermal Processes Laboratory Technopole de Borj-Cédria, BP : 95, Hammam Lif, Ben Arous, Tunisia.*

** Laboratory Smart Electricity & ICT, SEICT, LR18ES44, National Engineering School of Carthage, University of Carthage, Tunisia.*

Email 1 - safa.skouri@crten.rnrt.tn
Email 3 - salwa.bouadila@crten.rnrt.tn

1. Introduction

The adoption of renewable energy in the electricity sector is imperative for tackling the environmental and energy challenges of the 21st century. The economic dimension stands out as the most persuasive factor in the realm of any project or investment. As highlighted by the International Renewable Energy Agency (IREA), the amalgamation of various renewable energy technologies, including wind turbines, has the potential to reshape our energy landscape renewables energies [1], biomass and hydrogen energies, will provide over 60% of all global energy needs by 2050 [2]. However, all kinds of renewable energy plants need to be upgraded in all regions to meet the world energy transition. In this context, photovoltaic (PV) hybrid installations with energy storage play a crucial role in enabling a more efficient and stable utilization of solar energy. The optimization of excess solar radiation in greenhouses and the generation of electricity from renewable sources without negative effects on the environment remain the subject of intensive investigation [3]. Furthermore, arid and semi-arid regions are exceptionally well-suited for photovoltaic electricity production [4–6]. A significant research effort has been made in the field of energy to enhance the electrical and energy efficiency of greenhouses [7]. The estimation of photovoltaic energy requirements for a 150 m^2 greenhouse was conducted by Yildirim et al. [8]. They demonstrated that the photovoltaic greenhouse could meet 33 to 67.2% of the electricity demand, and the electrical energy generated by the photovoltaic system over a year is 21,510.4 kWh. Relevant works to meet the energy demand of greenhouse are developed [9–12] and to develop isolation material of greenhouses [13–15]. This study aims to present a thorough analysis of the electrical requirements of a hydroponic greenhouse and a PV/battery hybrid installation by combining the advantages of PV with energy storage capabilities, focusing on its performance and efficiency. The design of the PV/battery hybrid installation has been developed, with key components such as solar panels, inverters, batteries, and energy management devices described in detail. Criteria for component selection and design considerations to optimize the performance of a vertical greenhouse are also addressed. The performance of the PV/battery hybrid installation is evaluated in terms of energy efficiency, electricity production, battery utilization rates, and system stability.

2. Hydroponic greenhouse layout

The hydroponic greenhouse under investigation is a well-insulated structure with a galvanized framework covered by polyurethane sandwich panels, spanning an area of 24 m^2 and standing at a height of 3 m (Fig. 1). Comprising two distinct rooms facing southeast, this hydroponic greenhouse is meticulously designed to create an optimal environment for plant growth. The primary chamber is dedicated to hydroponics, while the smaller room serves as a space for

ISSN: 1737-9334

germination, as well as overseeing irrigation, ventilation, and conditioning processes. Within the main compartment, designated for plant cultivation, vegetation is arranged in rectangular trays set on a metal structure featuring five tiers spaced 0.5 m apart. This space incorporates two windows; one with single glazing on the north facade and another with double glazing on the south façade; totaling an area of 4.77 m², ensuring ample sunlight exposure on both sides. Addressing air renewal and ventilation, the soilless greenhouse is equipped with a ventilation system, comprising three fans strategically placed on both the north and south sides. Height lamps installed on all four walls serve as artificial lighting, compensating for insufficient sunlight in winter and ensuring adequate illumination. The greenhouse features an irrigation and water harvesting system that optimizes the supply of water and nutrient solutions essential for plant growth and metabolism acceleration. Drip irrigation is facilitated through pipes fixed on the trays, as detailed in Table 1 outlining the greenhouse equipment.

Table 1 Equipment used in the hydroponic greenhouse.

Equipement	Unit	Power (W)
AquaOxy aerator	2	60
NVF2-1.5/ TS4 inverter	1	900
Fan Type 1	2	250
Fan Type 2	1	50
Hunter X-core controller	1	10
Water pump	1	80
Centrifugal pump	1	370
Lamp	8	16
Chaine d'acquisition	1	20

Fig. 1. Experimental setup.

3. Results

3.1 Hydroponic greenhouse energy consumption

In ensuring the optimal functioning of the greenhouse, electric energy becomes a vital requirement, as all organisms depend on energy for their survival. The electrical energy consumption of the hydroponic greenhouse fluctuates based on the growth phase, the operational state of various equipment, and the specific needs of the vegetation. The power usage for different operations within the greenhouse throughout a barley growth cycle is

ISSN: 1737-9334

illustrated in Fig. 2. Ventilation, facilitated by two fans enhancing internal air quality, involves the continuous use of a inverter to modulate airflow velocity. Air renewal, occurring twice a day, requires 1400 Wh of energy. Lighting, crucial for the photosynthesis process, varies based on the cultivation phase, with an energy consumption of 128 Wh when all lamps are active. In terms of irrigation, Watering frequency adjusts throughout the growth cycle, with a maximum energy consumption of 90 W. Conditioning operations, essential for barley cultivation, encompass heating and cooling systems. The energy demand is 50 Wh during operation and 370 Wh at night. Fig. 3 provides an overview of the cumulative energy consumption required to sustain all operations within the hydroponic greenhouse throughout a barley cultivation cycle.

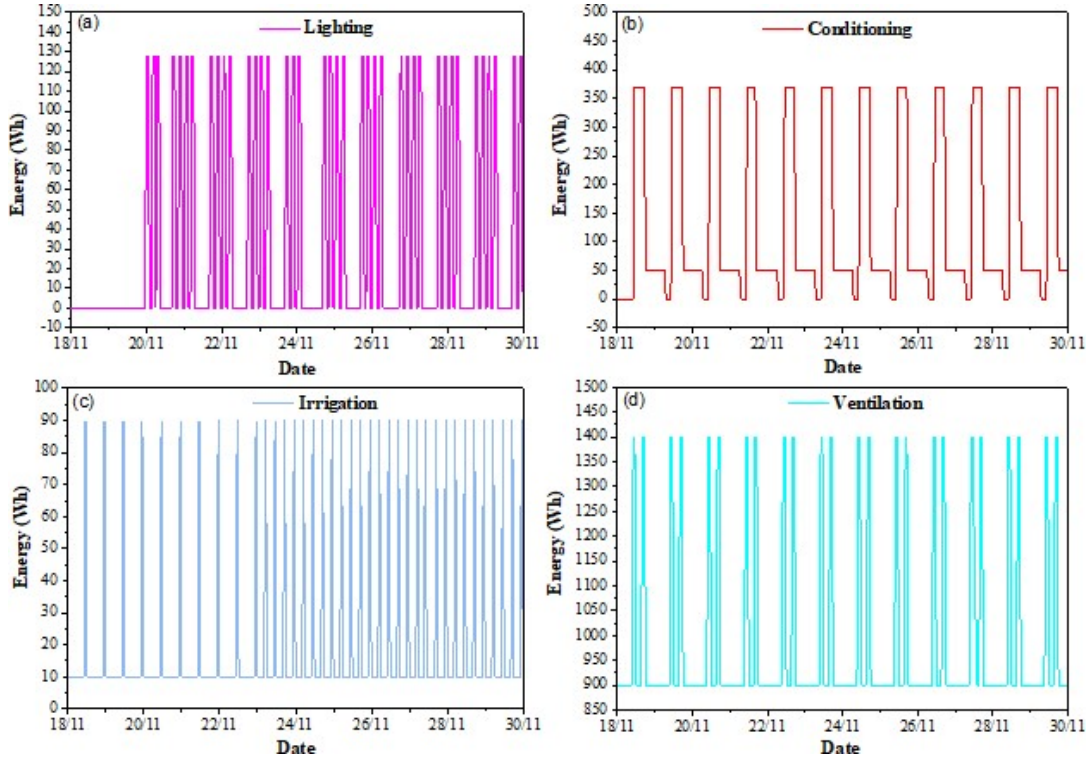

Fig. 2. Used power for HG operations.

ISSN: 1737-9334

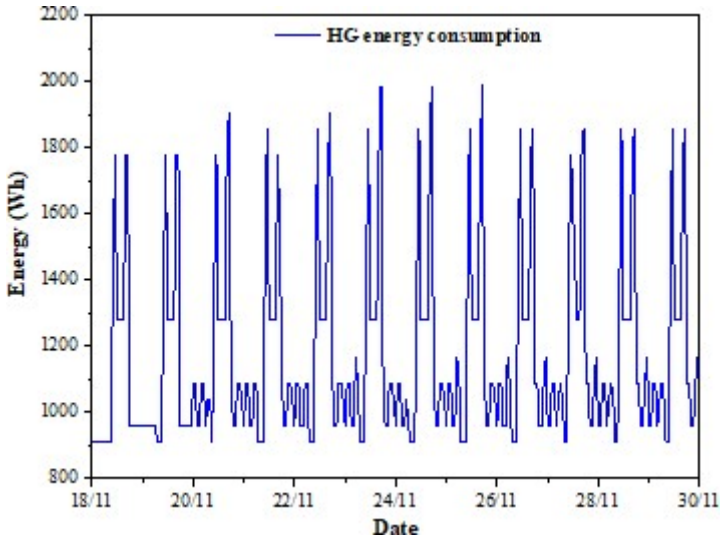

Fig. 3. HG electric energy consumption.

3.2 Photovoltaic system

As previously mentioned, crucial components within the hydroponic greenhouse rely on electric energy. Beyond the consumption of these devices, various factors must be considered, This factor accounts for meteorological uncertainties, the uncorrected inclination of modules based on the season, and the operational point of the modules. The photovoltaic (PV) system was meticulously sized and designed specifically for the hydroponic greenhouse, taking into consideration its electricity requirements. The peak power of the photovoltaic plant indicates that the energy demands of the greenhouse amount to 2.1 kWc. Consequently, all components of the PV system are proportionally dimensioned based on this output. While the plant will be connected to the grid, the inclusion of batteries ensures storage capability in the event of overproduction. Table 2 provides an overview of the components utilized in the PV/battery hybrid installation for the hydroponic greenhouse (Fig.4).

Table 2: Components of the hybrid PV/Battery installation.

Component	Units
Solar cell module 400Wc	8
Solar charge controller 30A	1
Inverter OFF GRID 24V/500VA	1
Solar battery 12V/200AH	4
Battery protection	1
DC protection box for a pre-wired chain with MC4	1

ISSN: 1737-9334

Fig. 4. PV installation.

3.3. Experimental analysis

The experimental analysis spanned a duration of 13 days, marked by significant fluctuations in irradiation ranging from 0 to 1033 W/m². Concurrently, ambient temperatures exhibited variability between 17.15 and 40.67 °C, as depicted in Fig 5(a). Fig. 5(b) and Fig.5(c) illustrate the generated voltage and current by the PV array. The current and voltage produced by the PV array exhibit a stable sinusoidal shape, reaching their peak values at 12 A and 167 V. Conversely, the grid voltage displays an unstable sinusoidal pattern, with maximum current values reaching 12 A.

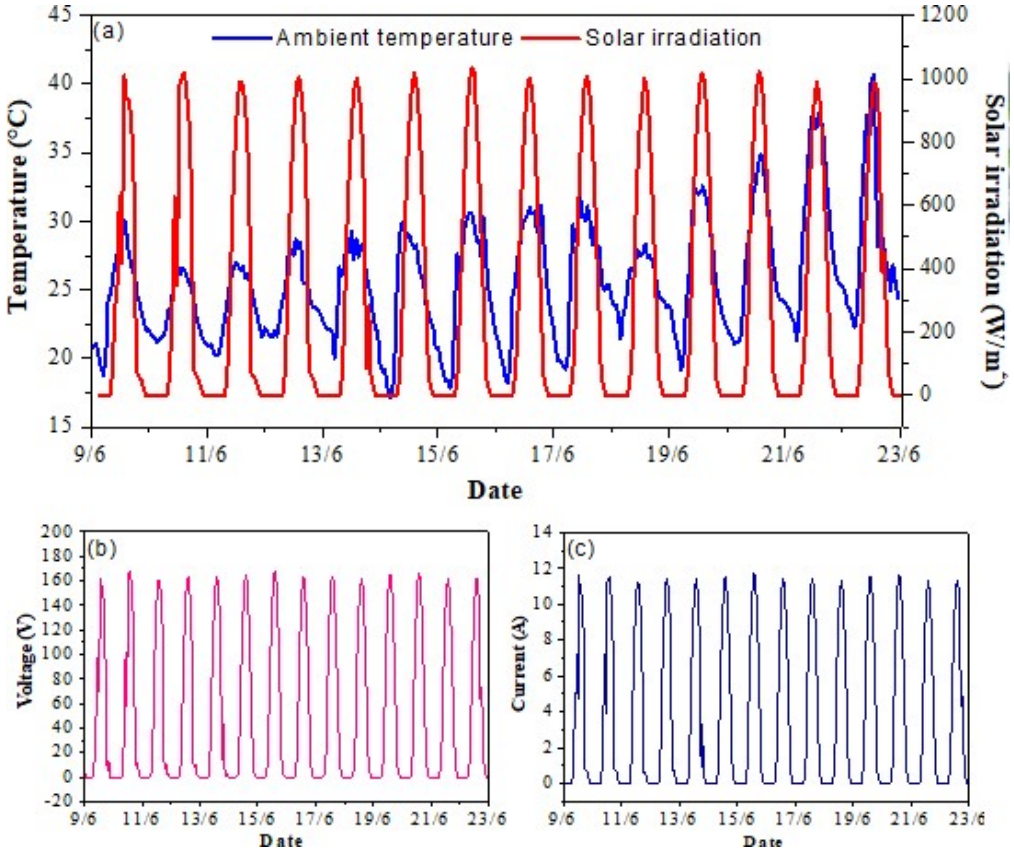

Fig. 5. Climatic conditions, generated voltage and current by the PV array

4. Conclusion

This study has underscored the significance of PV/battery hybrid installations as a sustainable energy solution. The in-depth analysis of the installation's performance and efficiency

ISSN: 1737-9334

highlights its potential to meet the electrical requirements of a hydroponic greenhouse while mitigating environmental impact. Consequently, this study contributes to advocating for the adoption of solar energy and energy storage in the global energy landscape, facilitating a transition toward a greener and more sustainable society.

References

[1] S. Skouri, A. Ben Haj Ali, S. Bouadila, S. Ben Nasrallah, Optical qualification of a solar parabolic concentrator usingphotogrammetry technique, Energy. 90 (2015) 403–416. https://doi.org/10.1016/j.energy.2015.07.047.

[2] J. Faraji, H. Hashemi-Dezaki, A. Ketabi, Multi-year load growth-based optimal planning of grid-connected microgridconsidering long-term load demand forecasting: A case study of Tehran, Iran, Sustain. Energy Technol. Assessments.42 (2020) 1–51. https://doi.org/10.1016/j.seta.2020.100827.

[3] A. Marucci, A. Cappuccini, Dynamic photovoltaic greenhouse : Energy efficiency in clear sky conditions, 170 (2016)362–376. https://doi.org/10.1016/j.apenergy.2016.02.138.

[4] M. Cossu, A. Cossu, P.A. Deligios, L. Ledda, Z. Li, H. Fatnassi, C. Poncet, A. Yano, Assessment and comparison of the solar radiation distribution inside the main commercial photovoltaic greenhouse types in Europe, Renew. Sustain.Energy Rev. 94 (2018) 822–834. https://doi.org/10.1016/j.rser.2018.06.001.

[5] K. Ezzaeri, H. Fatnassi, R. Bouharroud, L. Gourdo, A. Bazgaou, A. Wifaya, H. Demrati, A. Bekkaoui, A. Aharoune, C. Poncet, L. Bouirden, The e ff ect of photovoltaic panels on the microclimate and on the tomato production under photovoltaic canarian greenhouses, Sol. Energy. 173 (2018) 1126–1134.https://doi.org/10.1016/j.solener.2018.08.043.

[6] T. Alinejad, M. Yaghoubi, A. Vadiee, Thermo-environomic assessment of an integrated greenhouse with an adjustable solar photovoltaic blind system, Renew. Energy. 156 (2020) 1–13. https://doi.org/10.1016/j.renene.2020.04.070.

[7] E. Barbera, E. Sforza, L. Vecchiato, A. Bertucco, Energy and economic analysis of microalgae cultivation in a photovoltaic-assisted greenhouse : Scenedesmus obliquus as a case study, Energy. (2017). https://doi.org/10.1016/j.energy.2017.08.069.

[8] N. Yildirim, L. Bilir, Evaluation of a hybrid system for a nearly zero energy greenhouse, Energy Convers. Manag. 148 (2017) 1278–1290. https://doi.org/10.1016/j.enconman.2017.06.068.

[9] S. Bouadil, S. Skouri, S. Kooli, M. Lazaar, A. Farhat, Solar energy storage application in Tunisian greenhouse by means of phase change materials, 2014 Int. Conf. Compos. Mater. Renew. Energy Appl. ICCMREA 2014. (2014) 0–3. https://doi.org/10.1109/ICCMREA.2014.6843795.

[10] S. Bouadila, S. Skouri, S. Kooli, M. Lazaar, A. Farhat, Experimental study of two insulated solar greenhouses one ofthem use a solar air heater with latent heat, in: 2015 6th Int. Renew. Energy Congr. IREC 2015, 2015. https://doi.org/10.1109/IREC.2015.7110873.

[11] S. Bouadila, S. Baddadi, S. Skouri, R. Ayed, Assessing heating and cooling needs of hydroponic sheltered system in mediterranean climate: A case study sustainable fodder production, Energy. 261 (2022) 125274. https://doi.org/10.1016/j.energy.2022.125274.

[12] S. Bouadila, S. Baddadi, T.- Rehman, R. Ayed, Experimental investigation on the thermal appraisal of heat pipe-evacuated tube collector-based water heating system integrated with PCM, Renew. Energy. (2022). https://doi.org/10.1016/J.RENENE.2022.09.004.

[13] A. Dellagi, R. Ayed, S. Bouadila, A. Guizani, Study of the thermal behavior of a heated brick containing a phase change material, 2022 13th Int. Renew. Energy Congr. IREC 2022. 1 (2022) 5–9. https://doi.org/10.1109/IREC56325.2022.10002002.

[14] R. Ayed, S. Baddadi, A. Dellagi, S. Bouadila, M. Lazaar, Thermal behavior improvement of building materials using expanded polystyrene, 2022 13th Int. Renew. Energy Congr. IREC 2022. (2022) 1–4. https://doi.org/10.1109/IREC56325.2022.10002016.

[15] R. Ayed, S. Baddadi, S. Bouadila, S. Skouri, M. Lazaar, Architectural Development of the Buildings' Envelope to Improve Energy Efficiency, in: Adv. Sci. Technol. Innov., Springer International Publishing, 2022: pp. 459–461. https://doi.org/10.1007/978-3-031-00808-5_105.

ISSN: 1737-9334

Contribution to the characterization of blast furnace slag

Hazem MERADI[#1], Atmen Boukari[#2]

[#]*Research Center in Industrial Technologies CRTI, P.O. Box 64, Cheraga 16014, Algiers Algeria*

[1]h.meradi@crti.dz

[2]a.boukari@crti.dz

Introduction:

The production of steel is accompanied by the formation of solid or liquid by-products (about 550 kg per ton of steel). This represents approximately 17 million tons per year[1]. These by-products are extremely varied: slags of blast furnace and steel-works, calamines, muds and dust of de-dusting of smoke. Blast furnace slags are by-products of the steel industry. They are generated during the production of steel, during the development stage cast iron from iron ore. According to the cooling process of the molten slag, we distinguish two families[2-8]:

– Crystallized slag, obtained by slow cooling which transforms it into an artificial,

chemically stable hard rock;

– Vitrified slag, obtained by brutal cooling, generally with water, which gives it a .

vitreous structure allowing it to develop properties properties similar to those of cement.

Blast furnace slag is a byproduct of iron and steel production. Its physicochemical characteristics are influenced by the type of production process used. Depending on the iron and steel production processes and the raw materials, the chemical composition and solidification structure of the blast slag can vary[9-12].

There are three main types of iron and steel slag:

- Blast furnace slag,
- Conversion steel slag,
- Electric steelworks slags.

In our study we are interested in the characterization of slag, for various practical use.

Production of Slag furnace

As with most industrial by-products, the valorization of slag responds to:

- has a double challenge
- environmental, by avoiding the final storage of materials which still have waste status
- by offering less expensive solutions than other natural materials available.

ISSN: 1737-9334

We observed two type of slag:

- Crystallized slags:

They have physical and mechanical characteristics comparable to those of natural materials. They are used in technical road from the constitution of embankments, to the layers of road surface. Freshly produced slag and stocks called “slag”, built up over decades, are exploited asnatural rock quarries for the manufacture of aggregates.

- Vitrified slags:

Most often produced in the form of granulated slag, they find, due to their physicochemical characteristics, a privileged employment in the cement industry, but also as binders in different granular mixtures of road bases.

The slag production process in the blast furnace is illustrated in figure 1.

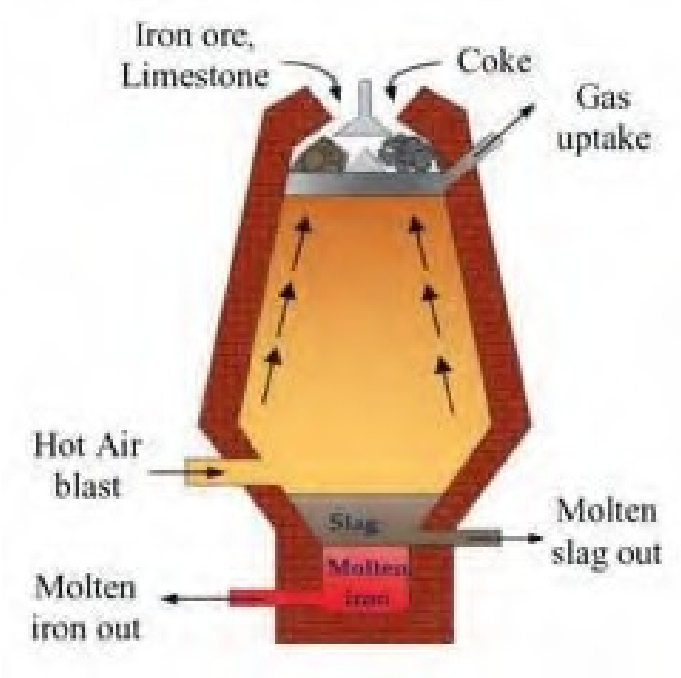

Figure 1: Process production of slag in Blast furnace[13]

Resultats of caracterization:

Chemical analysis of blast furnace slag sample were conducted using X-ray fluorescence (XRF) and presented in Table 1. The result shows the predominance of silica and lime with alumina and iron oxide in lower proportion.

Element	Mass %
CaO	38.5
Al_2O_3	7.6
SiO_2	42.8
Fe_2O_3	1.51
MgO	3.45
MnO	3.25
K_2O	0.4
Na_2O	0.7
Others	1.79

Table 1. Chemical composition of Blast furnace slag sample.

In order to follow the thermal behavior of the blast furnace slag powder at different temperatures, thermal analysis by Differential Scanning Calorimetry (DSC) and thermogravimetric (ATG) was carried out using a fully computerized Netzsch STA 409 PC. About 10 mg of powder was placedinto Al_2O_3 crucible and was heated at a rate of 10°C/min, from room temperature to 1100°C in a static air environment. Results obtained are showed in figure 1 for Differential Scanning Calorimetry and figure 2 for Thermogravimetric analysis.

ISSN: 1737-9334

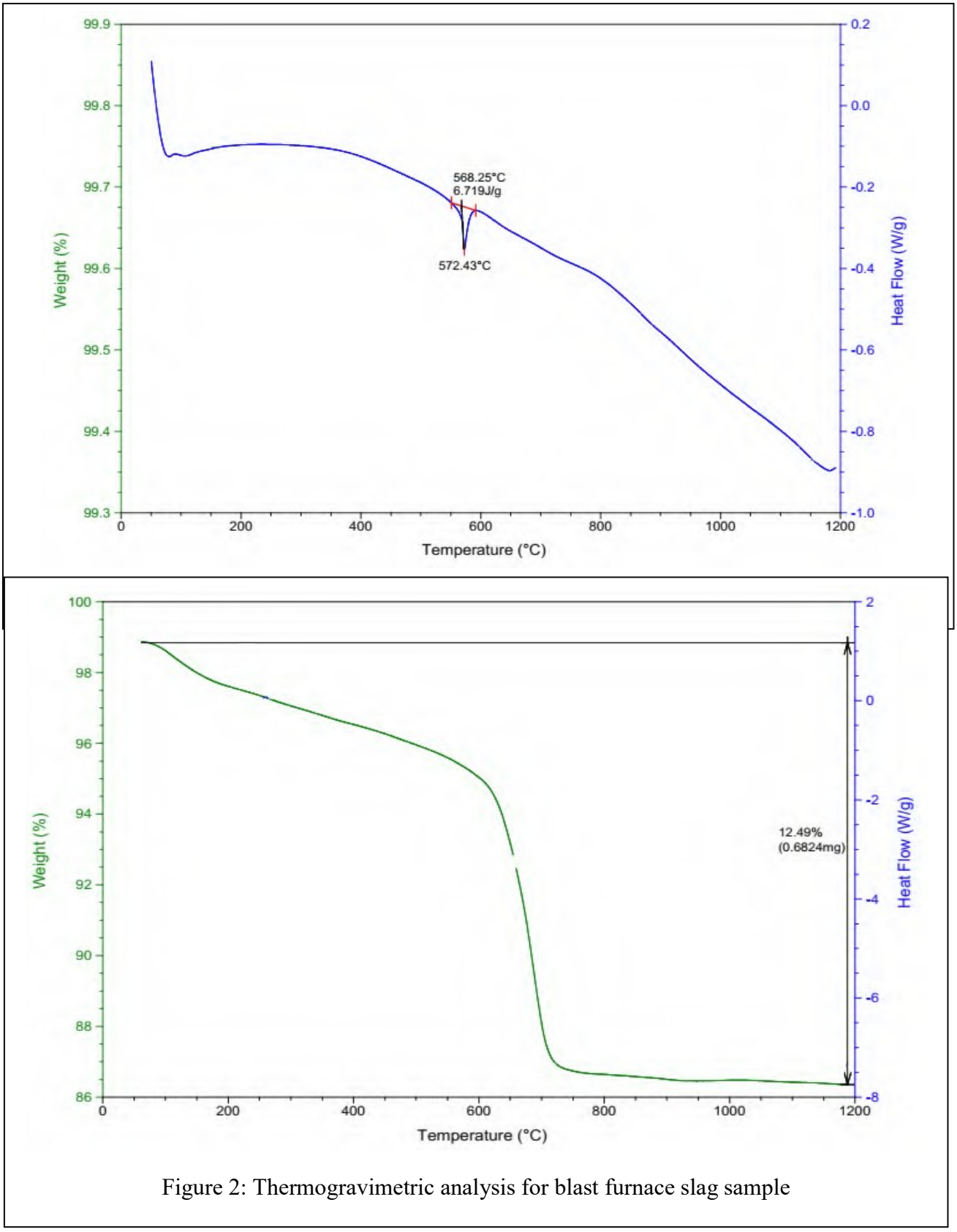

Figure 2: Thermogravimetric analysis for blast furnace slag sample

ISSN: 1737-9334

Conclusion:

The results of chemical analysis shows the predominance of silica and lime with alumina and iron oxide in lower proportion.

We can see from DSC spectrum three endothermic peaks at 75°C, 100°C and 572.43°C, and one Exothermic peak at 80°C shows in figure 1. The endothermic peak centered at 75°C and a shoulder around 100°C was assigned to the loss of water absorbed on the diatomite. The small peak at 572.43°C might be due to the quartz transformation.

The mass losses observed by thermogravimetric analysis and presented in figure 2 are 12%.

References :

[1] Jean-Marie Delbecq; Valorisation des co-produits issus de la fabrication de l'acier; actualité chimique - novembre 2009 - n° 335

[2] P. Williams and J. Quin, "The Use of Slag Characterisation to Monitor Steelmaking Processes with Particular Reference to Metallurgical Control and Refractory Performance," SEAISI MALAYSIA Conference, 1986.

[3] J.S. Soady, P.Williams, and D. Taylor, "Optimised Refractory-Compatible Practices for Secondary Ladle Processes," Personal Communication.1. F.A. Kemeny and D.J. Sosinsky, "Synthetic Ladle Slag Engineering for Improved Chemistry and Ladle Life," 48 th Electric Furnace Conference, 1990.

[4] M.A. Orehoski, "Ladle Refining Processes," Iron and Steelmaker, January, 1986.
F.A. Kemeny and D.J. Sosinsky, "Synthetic Ladle Slag Engineering for Improved Chemistry and Ladle Life," 48 th Electric Furnace Conference, 1990.

[5] G.A. Faulring, "Effect of CaC_2 on furnace slag," 49 th Electric Furnace Conference, 1990.
R.J. Fruehan and E.T. Turkdogan, "Physical chemistry of iron and steelmaking," Making, shaping, and Treating of Steel. U.S. Steel, New Edition 1981.

[6] J.A. Duffy and M.D. Ingram, The behaviour of basicity indicator ions in relation to the ideal optical basicity of glasses. Physics and Chemistry of glasses, 16, (1975).

[7] J.A. Duffy and M.D. Ingram, An interpretation of glass chemistry in terms of the optical basicity concept. Journal of non-crystalline solids, 21, (1976).

ISSN: 1737-9334

[8] J.A. Duffy, M.D. Ingram, and I.D. Somerville. Acid-base properties of molten oxides and metallurgical slags. Journal of chemical society, Faraday Transactions I, 74, (1978).

[9] Blanca Gill et al.; Chemical and microstructural characterization of blast furnace slag; Rev. Soc. cient. Parag. 2020;25(2):101-110

[10] Alexandre J., Sebileau J.L, 1988. « Le laitier de haut-fourneau : élaboration, traitements propriétés, emplois. » C.T.P.L. (Ed), Paris, France, 340 pages.

[11] Bruncher P., 2002. « Des laitiers cristallisés de haut-fourneau pour un pont en Moselle. Laitiers sidérurgiques n°82 (Ed.), France, Juin, pp 8-22.

[12] Martins, 2003.. « Demande d'autorisation de la société Granufos. » Rapport de l'Ingénieur de l'Industrie et des Mines Bordereau préfectoral N°50-2002 A.

[13] Pierre ROSSI and al. ; Blast furnace slags Origin, production and characteristics, Techniques de l'Ingénieur; Fevrier 2014

.

ISSN: 1737-9334

ISSN: 1737-9334